AD-A056 518 AIR FORCE INST OF TECH WRIGHT-PATTERSON AFB OHIO SCH--ETC F/G 9/4
QUADRATURE CLOCK MODULATION VERSUS BINARY AND QUADRATURE PHASE --ETC(U)
DEC 77 G A WHITE
UNCLASSIFIED AFIT/GE/EE/77-37 NL

1 OF 1
AD
A056 518

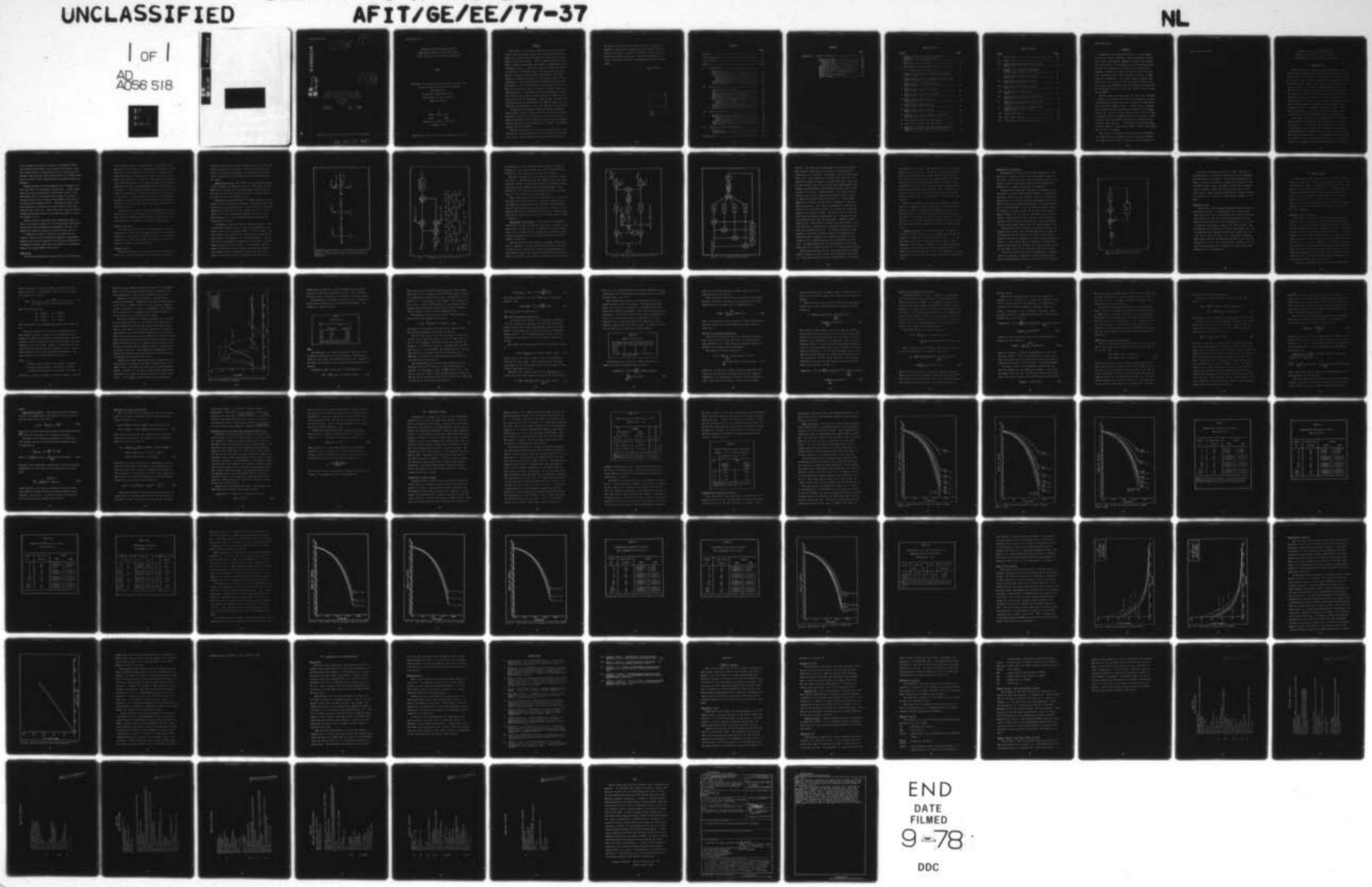

END
DATE
FILMED
9-78
DDC

AFIT/GE/EE/77-37

LEVEL II

AD A056518

AD No.
DDC FILE COPY

QUADRATURE CLOCK MODULATION VERSUS BINARY AND QUADRATURE PHASE SHIFT KEYING IN THE PRESENCE OF INTERSYMBOL INTERFERENCE

THESIS

AFIT/GE/
EE/77-37

Gary A. White
Capt USAF

78 07 07 013

AFIT/GE/EE/77-37

QUADRATURE CLOCK MODULATION VERSUS BINARY AND QUADRATURE PHASE SHIFT KEYING IN THE PRESENCE OF INTERSYMBOL INTERFERENCE

THESIS

Presented to the Faculty of the School of Engineering
of the Air Force Institute of Technology
Air University
in Partial Fulfillment of the
Requirements for the Degree of
Master of Science

by
Gary A. White, B.S.
Capt USAF
Graduate Electrical Engineering

December 1977

Preface

This thesis is the result of an investigation of quadrature clock modulation (QCM) versus binary and quadrature phase shift keying (BPSK and QPSK) in the presence of intersymbol interference (ISI). QCM is a modification of normal BPSK in which the alternate data bits are transmitted on an orthogonal carrier. QCM, when compared to BPSK, was found to improve the data performance of a communication system which is limited by intersymbol interference. QCM, when compared to QPSK, was found to be slightly inferior in data performance. The carrier tracking characteristics of QCM and BPSK were also investigated in the presence of ISI, and QCM was found to have the same carrier tracking characteristics as BPSK. In addition, the energy penalty for tracking a QPSK signal versus a binary modulated signal was obtained under no ISI conditions. This penalty, together with the almost equal data performance of QCM and QPSK, suggest that QCM could possibly be used as a back-up system to QPSK.

I would like to thank my committee members, Captains Gregg Vaughn and T.R. Hadley, for their valuable assistance and advise rendered to me during my work on this thesis. I would particularly like to thank my thesis advisor, Captain Stanley Robinson, for the enthusiasm, guidance, and valuable insight that he provided.

None of this thesis could have been accomplished if not for the love and consideration that I received from my family. First, to my sons Allen and David, who kept the TV

low during the early evening hours, thanks. Finally, but foremost, I would like to thank my wife, Bernice, for her total unselfishness in putting my academic needs first for the past two-and-a-half years. This has allowed me to achieve a personal goal that I have wanted for almost twenty years.

Gary A. White

Contents

Contents

List of Figures

List of Tables

Abstract

Quadrature Clock Modulation (QCM) is a binary phase shift keying (BPSK) technique in which alternate bits are transmitted orthogonally. Compared to normal BPSK modulation, QCM improves the performance of a communication system which is limited by intersymbol interference (ISI). Compared to quadrature phase shift keying (QPSK) for the same information rates, QCM is slightly inferior in data detection performance. The average carrier tracking capability of a QCM scheme is equal to that of BPSK for the same closed-loop bandwidth and time bandwidth product (BT) of the channel filter at a specified signal energy to noise ratio (Eb/No).

The data detection performance for QCM, BPSK, and QPSK is analyzed by comparing the one-shot probability of error conditioned on a phase error as a function of Eb/No and BT for a specified channel filter. Carrier tracking performance for QCM and BPSK is analyzed by obtaining an average phase error variance for the linear model of a Costas loop. In computing both the probability of error and phase error variance, the intersymbol interference is modeled from a truncated data sequence. In addition, the bit energy penalty for tracking a QPSK signal versus a BPSK or QCM signal with no ISI is examined.

QCM offers an advantage in data detection performance over BPSK for low BT products, and an apparent advantage over QPSK in better carrier tracking in the presence of a

noisy reference signal.

QUADRATURE CLOCK MODULATION VERSUS
BINARY AND QUADRATURE PHASE SHIFT KEYING
IN THE PRESENCE OF INTERSYMBOL INTERFERENCE

I. Introduction

The probability of error of a data communication system can be made arbitrarily small given enough signal energy or signal duration. However, in the real world, the constraints of limited signal energies, increasing information rates, and finite bandwidths place upper limits on the performance that can be obtained. In satellite communications, data rates must be high because of the large volume of information that is transmitted. Also, the frequency allocations for a system place a definite limit on the channel bandwidths that can be used. This two-pronged constraint of increasing data rates and fixed channel bandwidths becomes manifest in a phenomena known as intersymbol interference (ISI). Therefore, alternative signalling schemes must be sought that yield the best system performance for the lowest cost.

Intersymbol interference is caused by passing a data sequence through a filter of finite bandwidth. This effect can usually be neglected when the bandwidth of the filter is much larger than the data rate. However, as the data rate approaches the bandwidth of the filter, the effects of ISI become more pronounced. The degrading effects from ISI are twofold. First, the power is reduced in a given datum epoch by the smearing and distortion caused by the filter.

If not compensated with an increase in transmitter power, the resulting performance of the system will suffer. Second, reinforcement or cancellation of the desired decision variable from the other data pulses occurs on a random basis. The net result of this random process is reduced system performance.

Various methods have been employed in an attempt to reduce the effect of intersymbol interference. Linear equalizers can reduce intersymbol interference; however, some additional noise is introduced that reduces the total effective signal-to-noise ratio of the channel below that of an ideally wide channel (Ref 1). Nonlinear decision feedback equalizers introduce less noise; however, they only consider past data bits. Other techniques, such as partial response and coding schemes, have also been used to reduce the effects of ISI.

Another method, quadrature clock modulation (QCM), in which the alternate data bits of a binary phase shift keyed (BPSK) system are transmitted orthogonally, has been suggested as a means to reduce the effects of ISI (Ref 2).

A comparison of QCM to BPSK has been made (Ref 3). However, because of the increasing emphasis on multiphase systems and since QCM requires the additional complexity of a quadrature channel, QCM should be compared to quadrature phase shift keying (QPSK) (Ref 4:333).

Background

The Defense Communication Agency (DCA), the directorate

of the Defense Satellite Communication System (DSCS), has proposed QPSK and BPSK as the modulation techniques for DSCS Phase III. The system will utilize surface acoustic wave (SAW) filters with a combined receiver and transmitter bandwidth time product of 1.0 (Ref 5). The impulse characteristics of the SAW filters is roughly equivalent to a five-pole Butterworth filter. Nielsen modeled these system filters as a six-pole, 0.1 dB ripple Chebyshev bandpass filter and evaluated the performance of BPSK versus QCM for BT products of 0.5, 1, and 1.5. Because BPSK is essentially the back-up modulation scheme for DSCS-III, QCM should also be compared to QPSK to see if any improvement can be made in reducing the effects of ISI.

In addition, the carrier tracking performance for a QCM system has not been investigated. It is not known if this will introduce additional problems beyond the carrier tracking difficulties encountered in a BPSK or QPSK system.

Problem Statement

The purpose of this thesis is to determine the relative performance of BPSK, QCM, and QPSK under time and bandwidth constraints that produce significant amounts of intersymbol interference; and to investigate the carrier tracking performance of QCM versus BPSK and QPSK.

Problem Analysis

The problem analysis is divided into three general areas. First, the system description of the signal set and data

detection and carrier tracking components for the three modulation schemes are discussed. Second, the various viewpoints of analyzing intersymbol interference are examined. Third, the scope and limitations of the problem resolution are stated.

System Description: The signal sets for the three modulation schemes are shown in Figure 1. The signal set for QPSK can be thought of as two independent binary channels. For this reason, QPSK has half the data or symbol bandwidth of BPSK for the same information rate.

Quadrature clock modulation is a binary modulated transmission scheme in which the alternate data symbols are transmitted on an orthogonal signal. Thus, QCM has the same data bandwidth as BPSK for the same information rate. In this thesis, a BT of 2α for QPSK corresponds to a BT of α for BPSK and QCM at the same information rates and using the same channel filters.

A modulation scheme for QCM is shown in Figure 2. The logical data sequence, the I signal, is transmitted alternately on the sine or cosine channel. For this thesis, the sine channel corresponds to the odd data pulses and the cosine channel corresponds to the even data pulses. Because the data is transmitted orthogonally, the effects of intersymbol interference are reduced. In particular, the adjacent interference of the previous and past data pulses are transmitted on an orthogonal carrier and are not apparent to the data detector if perfect phase coherence can

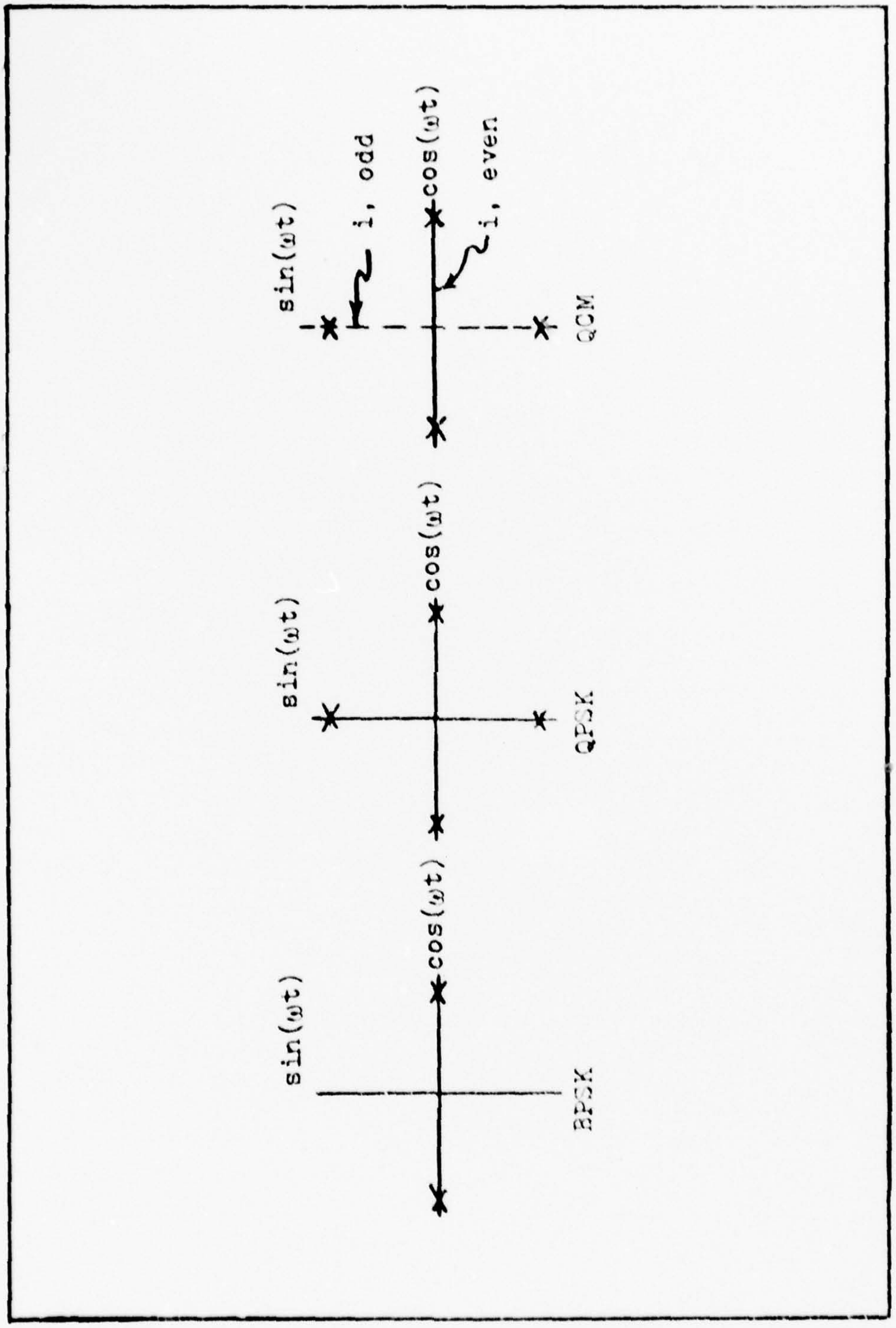

Fig. 1. Signal Set for Binary Phase Shift Keying, Quadrature Phase Shift Keying, and Quadrature Clock Modulation

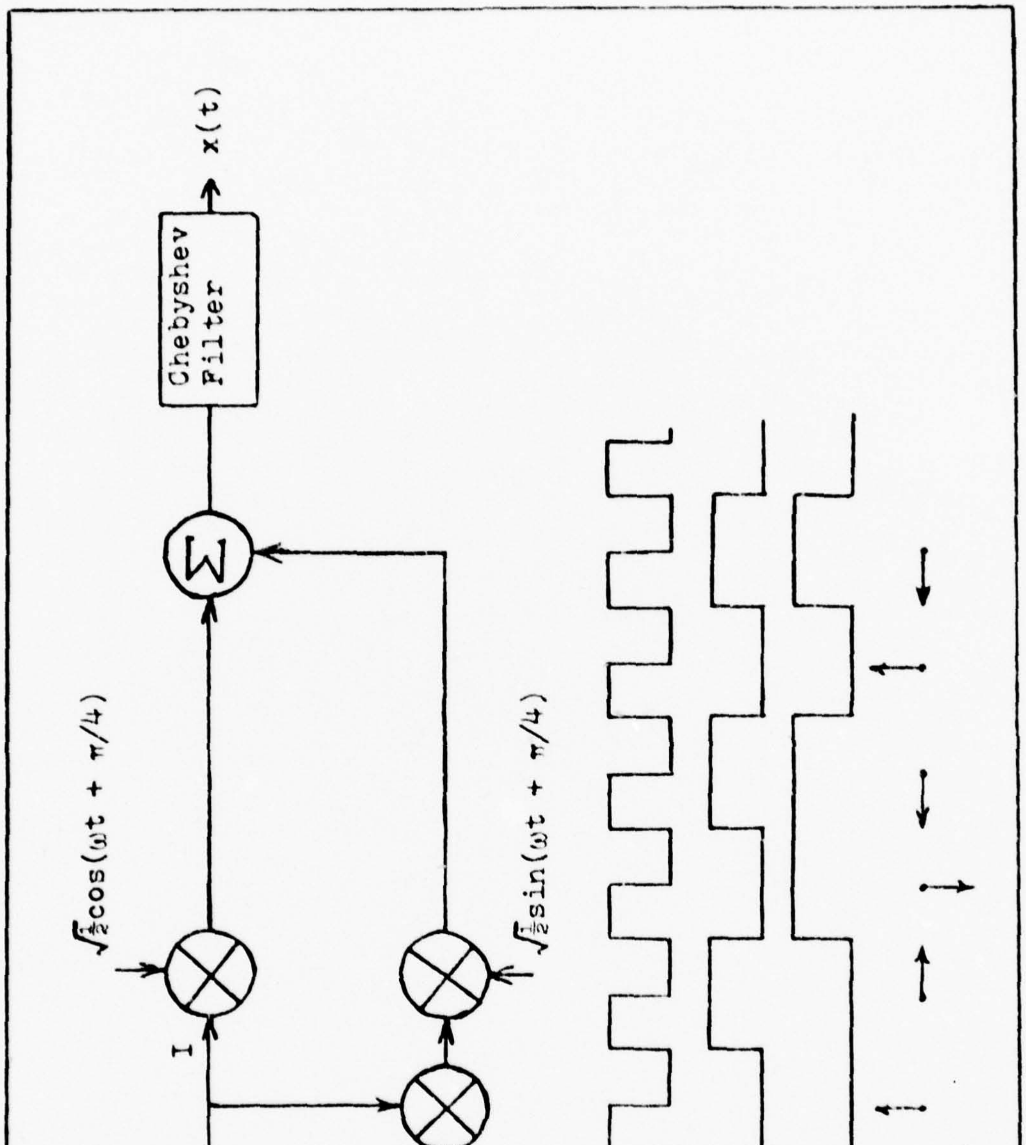

Fig. 2. Modulator Diagram for QCM (Ref 2)

be maintained. Even if perfect phase coherence cannot be maintained, the effects of ISI can still be significantly reduced for phase errors of less than $\pi/4$ radians.

The data detector for these modulation schemes is shown in Figure 3. For BPSK and QCM the output of the VCO is the reference signal. In the case of QCM, the reference signal is shifted by $\pi/2$ radians with every datum pulse. This clocking of the reference signal causes the data to always appear on the cosine leg of the Costas loop.

Since BPSK and QCM are binary modulated, the carrier can be tracked as shown in Figure 3. For QPSK, however, with its quadrature modulation set, a reference signal external from the data detector must be provided to resolve the modulation ambiguities and recover the carrier. A Costas loop that tracks a quadrature signal ($N = 4$ Costas loop) is shown in Figure 4.

Intersymbol Interference. The effects of intersymbol interference on data performance and carrier tracking is the main subject of this thesis. The problem of system evaluation is how to calculate the probability of error or carrier tracking parameters so as to include the effects of intersymbol interference.

For the data detection problem, the major efforts have been in two areas. First, various authors have attempted to find density functions or bounds on the probability of error which include the effects of intersymbol interference (Refs 6,7,8,9,10). Four types of bounds have been suggested

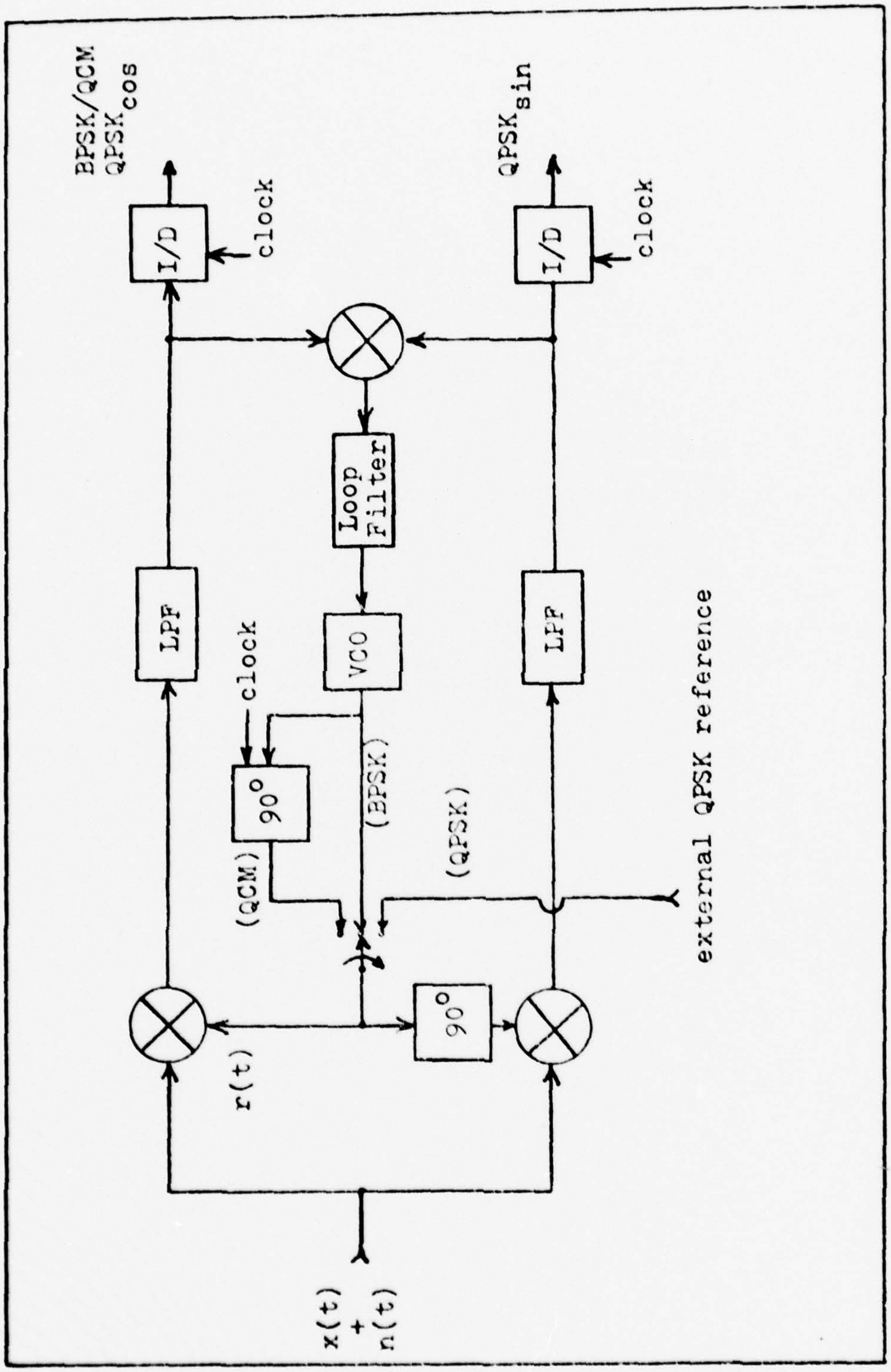

Fig. 3. BPSK/QCM/QPSK Costas Loop Receiver

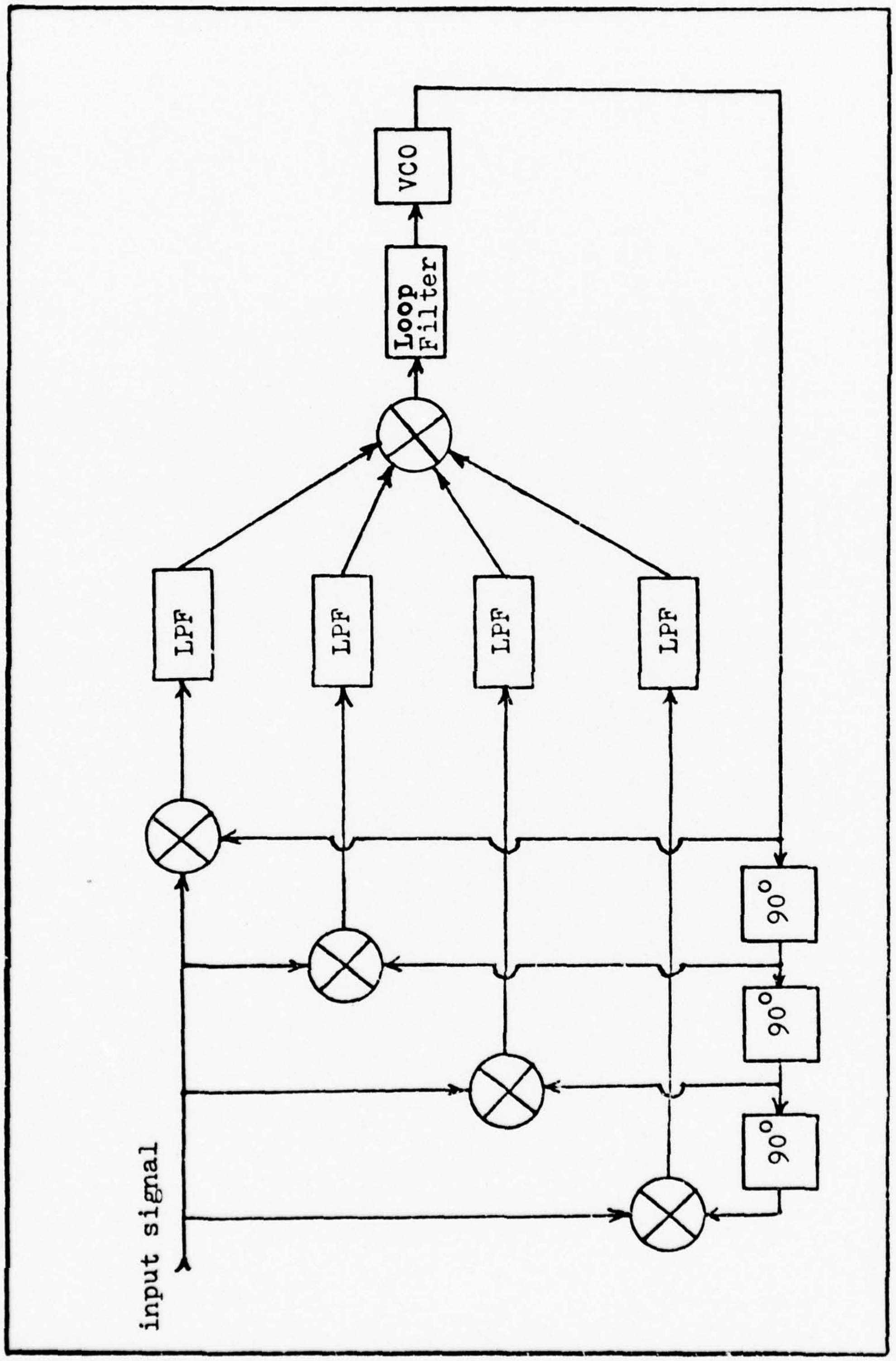

Fig. 4. N = 4 Costas Loop for QPSK

(Ref 9). The worst case bound assumes that all interferers add in phase; therefore, this bound is too pessimistic to represent a data detector. The second is the Chernoff bound (Refs 7,8). These bounds are difficult to obtain when the number of signalling phases is greater than four. Also, the Chernoff bounds tend to be a fairly loose approximation and become more inaccurate as the number of poles in the filter increases (Ref 9:51). Another method is by a pair of converging bounds where a lower and an upper bound are found in terms of marginal distributions (Ref 9). These paired bounds are difficult to obtain as the number of signalling phases increases. Also, they do not model or represent the errors due to crosstalk between the in-phase and quadrature channels that appear in QPSK. The fourth type of bound assumes that intersymbol interference can be treated as additive Gaussian noise with the same power. However, work by Shimbo, Fang, and Celebiler discount this last method. Density functions, approximating intersymbol interference, have also been generated (Ref 10). The density function method appears to have merit; however, based on observations of different pulse responses, this author questions the particular series representation of the intersymbol interference. It would appear that the coefficients in the series would have to be matched to the specific filter being modeled.

The second approach that has been suggested is to numerically calculate a finite number of interference terms (Ref 11). The major limiting factor in this method is the number

of computations increases exponentially as the level of modulation signals increase. The finite calculation method is also an approximation to an exact solution which contains an infinite number of terms. For BPSK and QPSK the combinatorial possibilities are within reason, and finite calculation will be used for this thesis. Also, this method of numerical simulation lends itself to easily evaluate an expression for the phase error variance of the BPSK or QCM carrier tracking loop in the presence of intersymbol interference.

With this method it is necessary to determine how many bits of a truncated sequence to include. Jones has found, except for small BT products, satisfactory results can be obtained with the adjacent intersymbol interference terms (Ref 11:126). For this thesis, the data stream will be truncated so as to include intersymbol interferers that are within a specified power threshold relative to the major datum pulse.

Problem Solution. The major objectives that will be resolved by this thesis are: (1) Compare BPSK to QCM for various BT products and signal-to-noise ratios. (2) Compare QPSK to QCM for the same information rates, filter bandwidths and transmitter powers. (3) Obtain expressions for phase error variance of a carrier tracking loop for BPSK and QCM in the presence of ISI. (4) Compare the energy requirements for the carrier tracking of QCM and BPSK versus QPSK.

Fundamental Assumptions

Assumptions must be made to narrow the problem to one which can be easily solved. Those assumptions global to the entire system are given here; assumptions needed to develop a specific equation or concept of the mathematical models will be stated as required in Chapter II.

Because data performance and carrier tracking are interrelated, an exact solution would require a simultaneous nonlinear analysis of the problem. However, for practical applications, the carrier tracking performance can be separated from the data detection problem. The basic assumption to this approach is that the carrier tracking device is initially in lock, at some offset phase error, and remains constant over the range of specified signal-to-noise ratios. Another way of stating this is that the carrier tracking device continues to track for a few dB of signal to noise degredation beyond which the data detector fails.

The data detector of Figure 3 is assumed linear so superposition is valid and a baseband model can be analyzed. The phase errors are assumed to be small so the carrier tracking loop can be replaced by a linear model as shown in Figure 5. Also, exact timing information is assumed for proper operation of the integrate and dump circuits and for the $\pi/2$ phase shift of the VCO output for QCM detection.

The noise process added to the signals prior to detection is a zero-mean, stationary, Gaussian random process with a two-sided power spectral density of No/2 (watts/Hz).

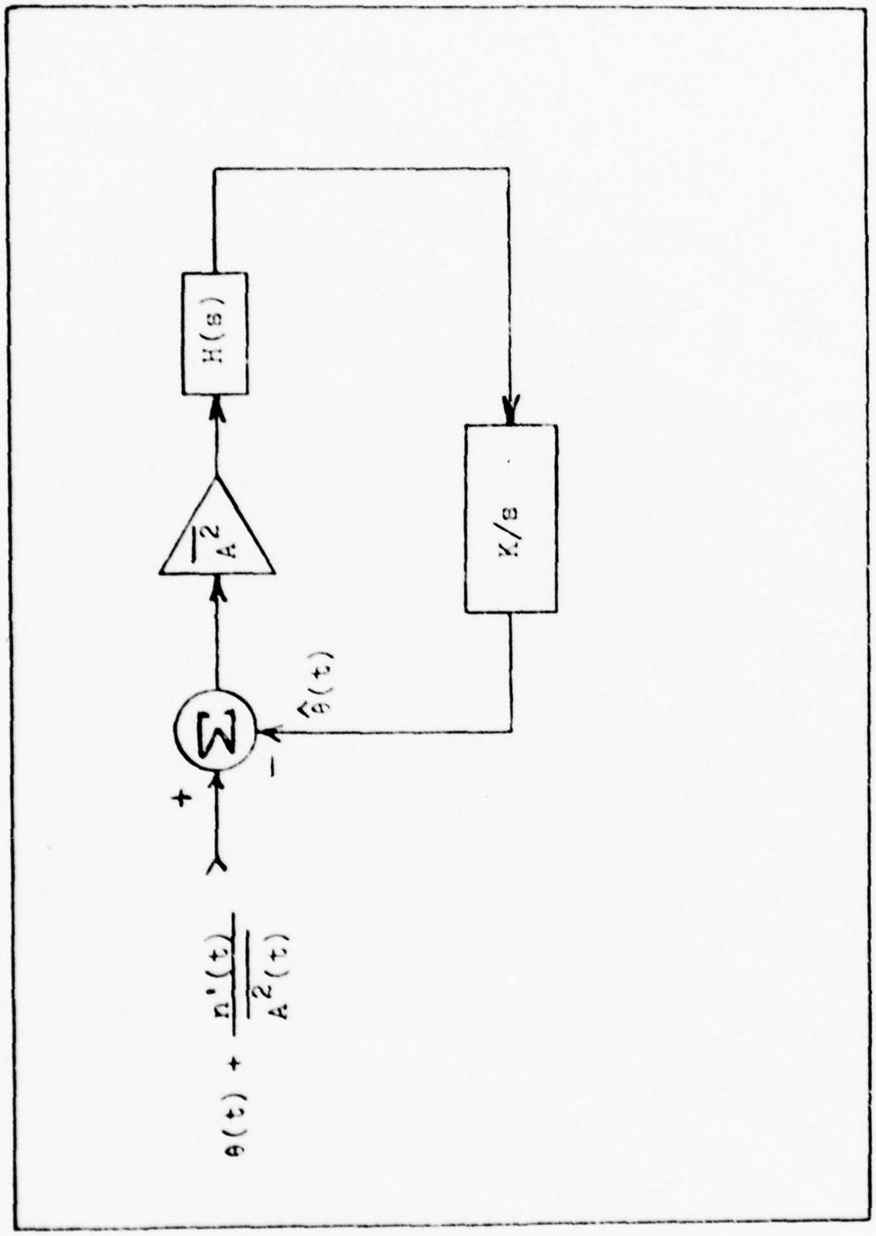

Fig. 5. Linear Baseband Model of
BPSK and QCM Carrier Tracking Loop

The final assumptions concern the data. Each bit of continuous data is assumed to be statistically independent and identically distributed. The one-shot probability of error is computed assuming an uncoded data stream for both the BPSK and QCM cases. For QPSK, a Gray code is assumed so as to compare a QPSK bit probability of error to the other cases. Also, any phase ambiguities in phase tracking are assumed to be resolved by differential encoding of the data.

Research Method

First, all of the necessary mathematical models will be developed to answer the major objectives of this thesis. These models will then be programmed for numerical analysis. Case results for data detection performances will be obtained for QCM versus BPSK for BT products of 0.5, 1.0, and 1.5 and with fixed phase errors of 0°, 10°, and 20°. QCM and QPSK will be compared at the same information rate, filter bandwidth and transmitter power for BT pairs of (0.5, 1.0), (0.75, 1.5), and (1.0, 2.0). The carrier tracking phase error variance for BPSK and QCM will be given for BT products of 0.5, 1.0, 1.5, and infinity. Finally, the carrier tracking penalty for a QPSK system under no ISI conditions will be investigated.

II. System Model

In this chapter the system model for evaluating the performance of BPSK, QCM, and QPSK is developed. First, a specific Chebyshev filter is described that will be used in the analysis of all three signalling schemes. However, the performance equations for BPSK, QCM, and QPSK derived in the presence of ISI contain a general filter term. The phase error variance for the $N = 2$ Costas loop is derived in the presence of ISI for both BPSK and QCM. Finally, the energy penalty for carrier tracking of a QPSK system versus BPSK or QCM is obtained.

Chebyshev Filter Response

The effects of intersymbol interference are characterized, in part, by the pulse responses $p(t)$ of the channel filters. The use of numerical analysis dictates a decision for the model of the filter. DCA has proposed a system that utilizes surface acoustic wave filters that have a response similar to a five-pole Butterworth filter. However, the impulse response of these filters was not available for use in this thesis. It has been shown that, in general, intersymbol interference increases with an increase in the number of poles for both Chebyshev and Butterworth filters (Ref 11). With the philosophy of obtaining a close upper bound by increasing the poles by one, Nielsen chose a six-pole Chebyshev filter to model the channel filter.

In order to correlate the results of this thesis with

those of Nielsen, the filter response that he chose will also be used here. The transfer function of the six-pole, 0.1 dB Chebyshev filter is

$$H(s) = \frac{Gb0}{s^6 + b5s^5 + b4s^4 + b3s^3 + b2s^2 + b1s + b0} \qquad (1)$$

where G is the gain and

$$b0 = 0.20713 \qquad b3 = 2.77908$$
$$b1 = 0.90176 \qquad b4 = 2.96575$$
$$b2 = 2.04784 \qquad b5 = 1.71217$$

and the frequency is in radian/second (Ref 12:290, Table A. 2).

The pulse response of the filter is obtained by using two computer programs. Factors of the denominator polynomial are obtained from POLY (a local polynomial evaluation routine). These factors are then used to evaluate the step-response H(s)/s with PARTL. PARTL is a local Heavyside partial fraction expansion and time response program. Both of these programs are briefly discussed in Appendix A. The step-response of the filter with unity gain is

$$\begin{aligned} r(t) = {} & 1.0 \\ & + 0.94211 \exp(-0.31334t) \sin(0.77339t + 116.168^\circ) \\ & + 0.25237 \exp(-0.11469t) \sin(1.0565t - 19.727^\circ) \\ & + 2.32050 \exp(-0.42806t) \sin(0.28310t + 229.341^\circ) \qquad (2) \end{aligned}$$

The pulse response is obtained from p(t) = A(r(t) - r(t-T)),

where A is the normalized voltage magnitude of the response and T is the pulse time duration; A will be varied to obtain appropriate signal to noise ratios for the plots.

Equation 2 is modified to obtain a step-response in terms of BT products. Applying the frequency scaling factor in the form $t = BT2\pi t'$, where t' is the new time variable, yields an expression in terms of BT products. The BT product is defined to be one when the one-sided bandwidth is one Hz and the pulse duration is one second.

The pulse-responses for three BT products for this filter are shown in Figure 6. This figure illustrates the increased distortion or spreading caused with lower BT products. Also apparent is the delay that must be applied to the integrate and dump circuits to maximize their outputs. This time or group delay can be obtained in a number of ways. Jones evaluated the derivative of the phase function of the filter (Ref 11:126, Eq 41). However, Hansell suggests the use of a finite difference method whenever a baseband model is employed (Ref 13). Both methods are suboptimum in obtaining the minimum error of probability because they fail to consider the nonlinear phase terms.

Nielsen integrated numerically with a constant one second interval in increasing increments along the pulse response until a time delay was found that yielded a maximum output. However, the time delays that Nielsen obtained for his filter are suspect by observation of his Figure 4 (Ref 3:20). It is surmised that Nielsen had an error in his

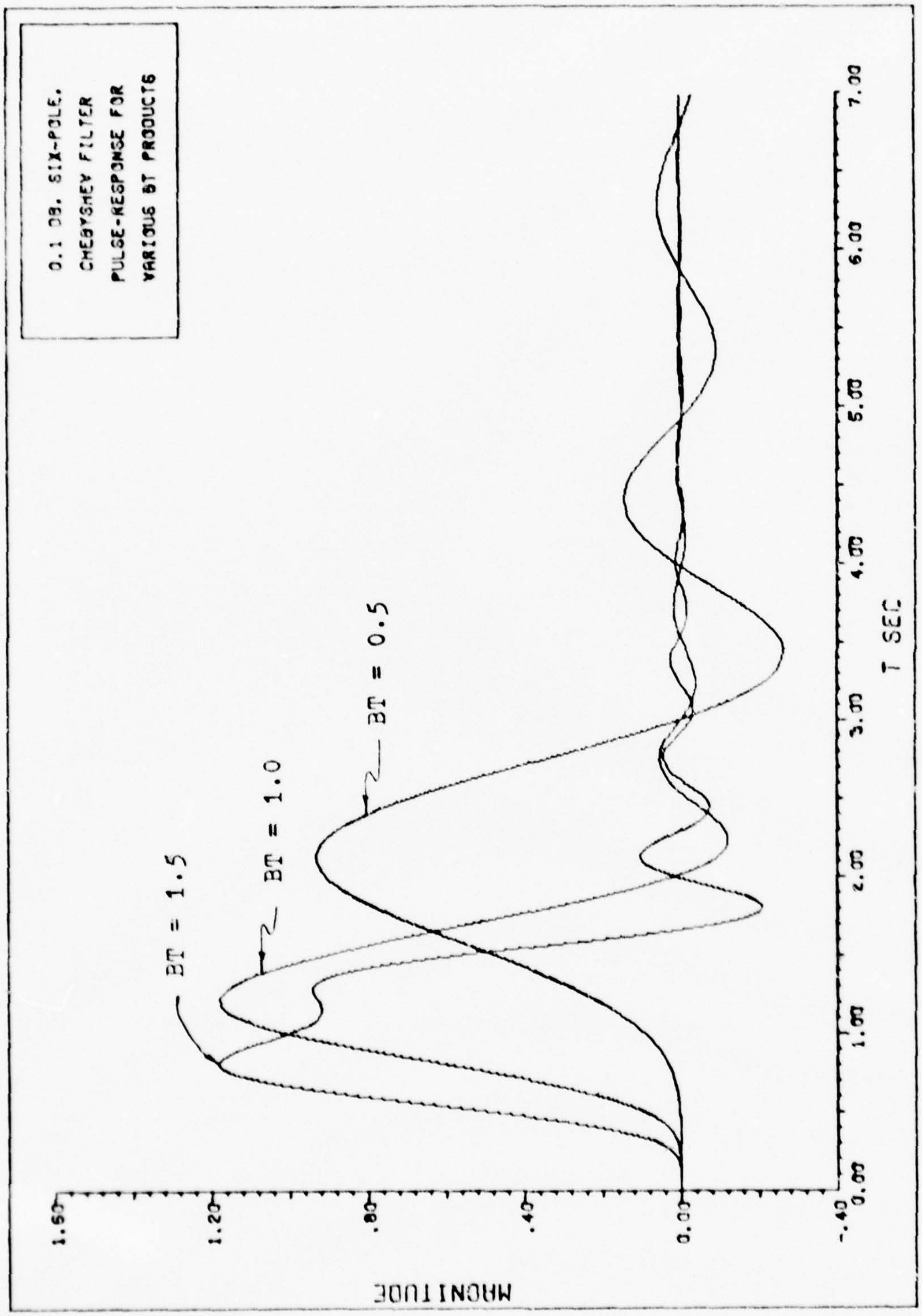

Fig. 6 Pulse-Response for a One-Second, One-Volt Input Pulse for Various BT Products

program which resulted in a narrow window of integration time rather than the one second interval. This is because his delay times correspond to the peak of the pulse-response.

By duplicating the method that Nielsen used, corrected values of time delays for this filter were obtained. The results are shown in Table I.

Table I

Filter Delay

BT	τ, sec Nielsens	Corrected
2.0	*	0.38
1.5	0.65	0.52
1.0	1.0	0.74
0.75	*	1.04
0.5	2.0	1.60

*Not computed (From Ref 3:19)

BPSK

The probability of error equation for BPSK with no intersymbol interference is first developed. Although this result is well known, the development serves as a blueprint for BPSK, QCM and QPSK in the presence of intersymbol interference.

Transmitted BPSK signals may be represented as

$$x(t) = \sqrt{P} \sum_i m_i(t-iT) \cos(\omega t + \theta(t)) \qquad (3)$$

where $m_i(t)$ is a T-second rectangular pulse of unit amplitude with sign $\pm$ 1 depending on the i^{th} data value, and $\theta(t)$ is a random process representing phase instabilities. For this thesis, T will always be one second. The received signal is $y(t) = x(t) + n(t)$, where $n(t)$ is zero-mean, white-Gaussian noise with power spectral density No/2 (watt/Hz) (Ref 4: Chapters 5,6) or (Ref 15: Chapters 1,4).

The baseband product of $y(t)$ and the cosine reference signal $r(t)$ after lowpass filtering is

$$y'(t) = \sqrt{P} \sum_i m(t-it) \cos\Phi(t) + n_1(t) \tag{4}$$

where $\Phi(t)$ is the phase error between the incoming phase $\theta(t)$ and the estimate of $\theta(t)$ made by the VCO.

The i^{th} data signal out of the integrate and dump (I/D) circuit is $d_i = \int_I (\cdot)dt$, where I is the i^{th} data time $iT + \tau$ to $iT + \tau + T$ seconds. For this thesis, the data will be obtained in the 0^{th} data interval. Assuming that the 0^{th} data bit $m_0 = 1$, and that $\Phi(t)$ is constant over the integration interval, the output from the I/D circuit is $d_0 = T\sqrt{P} \cos\Phi + N$, where N is a Gaussian random variable with zero mean and variance NoT/2.

The probability of a decision error, based on the hypothesis that the 0^{th} data bit is one and the phase is constant, is $P(\text{error}|m_0 = 1,\Phi) = P(T\sqrt{P} \cos\Phi + N < 0)$. But this is just the "tail" of the Gaussian density of the random variable N integrated from negative infinity to $-T\sqrt{P} \cos\Phi$. In terms of an error function complement

$$P(\text{error}|m_0 = 1,\Phi) = \frac{1}{2}\,\text{erfc}\left(\sqrt{\frac{PT}{No}}\cos\Phi\right) \tag{5}$$

The total probability of error conditioned on the phase error is then

$$P(\text{error}|\Phi) = \frac{1}{2}\,\text{erfc}\left(\sqrt{\frac{Eb}{No}}\cos\Phi\right) \tag{6}$$

for equal a priori probabilities.

BPSK with Intersymbol Interference

In the previous section, the conditional probability of error equation was developed for BPSK where the transmission filter was assumed wide relative to the data bandwidth. This assumption is no longer valid as BT products become smaller. *The i^{th} modulation pulse term, $m_i(t-iT)$,* is distorted and spread in time as it passes through the filter.

The input to the data detector with m interfering pulses is

$$y'(t) = \sqrt{P}\sum_m p(t-mT)\cos(\omega t + \theta(t)) + n(t) \tag{7}$$

where p(t) is the pulse-response of the filter convolved with the 0^{th} data pulse. This expression shows the additive nature of the intersymbol interference relative to the desired data epoch (m = 0).

With the sign of p(t) held positive, corresponding to a one being sent, the noiseless output of the I/D circuit is

$$S = \sqrt{P}T\cos\Phi\left[\int_I |p(t)|\,dt + \sum_{\substack{m\\ m\neq 0}} \int_I p(t-mT)\,dt\right] \tag{8}$$

where the last term represents an infinite summation of the interferers seen in the desired data epoch, and I is the 0^{th} interval from τ to $\tau + T$.

For computational purposes, a truncation of the m interfering data pulses is necessary. The number of future pulses (or bits) are determined by the group delay of the filter for a desired BT product. Past bits are contiguously included for the worst BT case until a power threshold relative to the desired data pulse is reached (20 dB down). Table II shows the past and future bits considered in the numerical computations for BPSK and QCM. The number of bits for the QPSK case is discussed in that section.

Table II

Number of Bits (KB)

BT	Past Bits (KP)	Future bits (KF)
0.5	7	2
0.75	7	2
1.0	8	1
1.5	8	1

KB = KP + KF

The probability of error for BPSK conditioned on a phase error and a truncated data sequence is

$$P(e|\Phi,\text{data}) = \frac{1}{2}\,\text{erfc}\left(\sqrt{\frac{Eb}{No}}\cos\Phi\left(\int_I |p(t)|dt + \sum_{\substack{m \\ m\neq 0}}^{KB} \int_I p(t-mT)dt\right)\right) \tag{9}$$

where the truncated summation includes only those KB interfering bits from Table II.

With the weak assumption that intersymbol interference and phase error are independent, the probability of error conditioned on the phase error is approximated as

$$P(e|\Phi) = \frac{1}{2^{KB}} \sum_{i=1}^{2^{KB}} P(e|\Phi, \text{data}_i) \tag{10}$$

where the conditioned error equation is summed and averaged over all possible bit combinations for a data stream of length KB + 1.

QCM with Intersymbol Interference

The received signal for QCM is an alternating quadrature signal that is binary modulated. The QCM signal is best represented as a BPSK signal in which the carrier is shifted by $\pi/2$ radians every datum pulse.

The input to the data detector is

$$y'(t) = \sqrt{P}\Big[\sum_{\substack{m \\ \text{even}}} p(t-mT)\cos(\omega t + \theta(t)) + \sum_{\substack{m \\ \text{odd}}} p(t-mT)\sin(\omega t + \theta(t))\Big] + n(t) \tag{11}$$

where p(t) is the pulse response resulting from the convolution of the desired datum pulse m(t) with the impulse-response of the transmission filter as in the previous section. The receiver of Figure 3, page 8, has a clocked

reference signal so as to always output the data on the cosine leg of the Costas loop; exact timing for the clock is assumed.

Again, with the sign of p(t) held positive corresponding to a one being sent, the noiseless output of the I/D circuit is

$$S = \sqrt{P}T[\cos\Phi(\int_I |p(t)| dt + \sum_{\substack{m \\ \text{even} \\ m \neq 0}} \int_I p(t-mT)dt) + \sin\Phi(\sum_{\substack{m \\ \text{odd}}} \int_I p(t-mT)dt)] \tag{12}$$

This equation, when compared to Eq 8, shows the reduction of the odd interferers relative to the desired datum epoch. This result, when compared with Eq 15 in Nielsen's thesis differs in the addition of the sinΦ term. This term was included because it represents the demodulation distortion caused by the sine channel when perfect coherent detection cannot be maintained. As the carrier tracking phase error increases to $\pi/4$ radians, the QCM signal from the I/D circuit degenerates to that of the BPSK case. The one-shot probability of error for QCM conditioned on a particular phase error and data sequence is

$$P(e|\Phi,\text{data}) = \frac{1}{2}\,\text{erfc}[\sqrt{\frac{Eb}{No}}\{\cos\Phi(\int_I |p(t)| dt + \sum_{\substack{m \\ \text{even} \\ m \neq 0}} \int_I p(t-mT)dt) + \sin\Phi(\sum_{\substack{m \\ \text{odd}}} \int_I p(t-mT)dt)\}] \tag{13}$$

QPSK with Intersymbol Interference

As shown in Figure 1, page 5, QPSK can be represented as two independent binary channels. The probability of a correct decision is $P(c|\Phi) = (1-P(e_c|\Phi))(1-P(e_s|\Phi))$, where e_c and e_s are the independent cosine and sine channel errors and where the phase error is the same for both channels (Ref 4:333-336). In writing this expression, it is assumed that the decision variables from the sine or cosine I/D circuits (d_s or d_c) are independent. This is valid since the noise variables N_1 and N_2 are uncorrelated Gaussian random variables; hence, they are also independent.

The signal input to the data detector is

$$y'(t) = \sqrt{P}[\sum_m p_c(t-mT)\cos(\omega t + \theta(t)) +$$

$$\sum_m p_s(t-mT)\sin(\omega t + \theta(t))] + n(t) \quad (14)$$

With the sign of the 0^{th} cosine datum pulse held positive, the output from the cosine I/D circuit is

$$d_c = \sqrt{P}T[\cos\Phi(\int_I |p_c(t)|dt + \sum_{\substack{m \\ m\neq 0}} \int_I p_c(t-mT)dt +$$

$$\sin\Phi(\sum_m \int_I p_s(t-mT)dt)] + N_1 \quad (15)$$

where the first term is the noiseless signal S_c from the cosine I/D circuit. Alternately, with the sign of the 0^{th} sine datum pulse held positive, $d_s = S_s + N_2$, and N_1 and N_2 are independent Gaussian noise terms with zero-mean and

variance NoT/2.

Writing the modulation set for the two independent channels as $m_c = \pm 1$ and $m_s = \pm 1$, where the subscripts c and s refer to the cosine or sine channel, the probability of an error for the cosine channel is $P(e_c|\Phi) = P(m_c = +1) \cdot P(e|m_c = +1, \Phi, \text{data}) + P(m_c = -1)P(e|m_c = -1, \Phi, \text{data})$. With m_c and m_s both being identically distributed, the one-shot probability of an error is

$$P(e_c|\Phi,\text{data}) = \frac{1}{2}\,\text{erfc}\Big[\sqrt{\frac{Eb}{No}}\,\{\cos\Phi(\int_I |p_c(t)|dt + \sum_{\substack{m\\m\neq 0}} \int_I p_c(t-mT)dt) + \sin\Phi(\sum_m \int_I p_s(t-mT)dt)\}\Big] \tag{16}$$

Averaging over all possible values of a truncated data sequence for both channels,

$$P(e_c|\Phi) = \frac{1}{2^{KB+1}} \sum_{i=1}^{2^{KB+1}} P(e_c|\Phi,\text{data}_i) \tag{17}$$

which, by symmetry, is also the probability of error for the sine channel. Using the equation for a correct decision, the probability of a total symbol error for QPSK conditioned on the phase error is $P(e|\Phi) = 2P(e_c|\Phi) - P^2(e_c|\Phi)$.

In order to make a fair comparison between QPSK and QCM, the symbol error for QPSK must somehow be related to the symbol error for QCM. If the QPSK symbols are encoded with a Gray code, then the bit error probability for QPSK is

$$P(e_b|\Phi) = P(e|\Phi)/\log_2 N \tag{18}$$

where N is number of QPSK symbols (four) and the symbol error is small (Ref 14:106). Since the symbol error for QCM is also the bit error, a common denominator now exists for a comparison of the two systems.

In order to numerically compute Eq 17 in a reasonable amount of time, the number of truncated bits considered in a channel must be reduced from those in the binary cases. The number of bits considered in Table II were determined from the worst case situation (BT = 0.5). Inspection of the pulse-response for the worst case for QPSK (BT = 1.0) shows that interferers within 30 dB can always be included for this filter when one future bit and three past bits are considered.

BPSK Carrier Tracking Performance

For a received BPSK signal plus noise as given in equation 3, the inputs to the multiplier prior to the loop filter in Fig. 3 are

$$A(t)\cos\Phi + n_1(t) \quad \text{(cosine leg)}$$
$$A(t)\sin\Phi + n_2(t) \quad \text{(sine leg)} \qquad (19)$$

where $n_1(t)$ and $n_2(t)$ are zero-mean independent Gaussian noise processes with variance NoB. And $A(t) = \sqrt{P}\Sigma p(t-mT)$ is the sum of all interfering pulses and data seen in the desired integration time, and is assumed to pass through the lowpass filters in the loop with no distortion. The two-sided bandwidth of the lowpass filter, 2B, is assumed to be one Hz so as to correspond to the bandwidth of a matched

filter for one second data pulses.

The output from the multiplier applied to the loop filter is

$$e(t) = \frac{A^2(t)}{2} \sin 2\Phi(t) + A(t) \cos\Phi(t) n_2(t) +$$

$$A(t) \sin\Phi(t) n_1(t) + n_1(t) n_2(t) \qquad (20)$$

where $\Phi(t)$ and $n_1(t)$ and $n_2(t)$ are independent of each other.

The last three terms represent the total effective noise signal $n'(t)$ which consists of additive Gaussian noise and intersymbol interference applied to the loop with an autocorrelation of (Ref 14:252 Eq 8.5.3)

$$R_{n'}(\tau) = R_{n_1}(\tau) R_A(\tau) + R^2_{n_1}(\tau) \qquad (21)$$

For phase errors that are small ($< 20^o$), $\sin 2\Phi$ of the signal term is well approximated by 2Φ, and the Costas loop can be represented as a linear system as shown in Figure 5, page 13. Inherent in writing the effective noise term at the input of the Costas loop are assumptions concerning the noise and phase error processes. In general, the noise process $n'(t)$ is a function of the phase error $\Phi(t)$; however, with $\Phi(t)$ assumed to be slowly varying with time (i.e. constant over several data intervals), $n_1(t)$ and $\Phi(t)$ can be shown to be effectively independent of each other (Ref 14:251) and (Ref 15:81 Eq 3-32). This allows the total effective noise $n'(t)$ to be superimposed back through the amplifier with an appropriate gain at the input of the loop.

Now $\overline{A^2(t)}$ represents the time averaging of the error signal over the coherence time of the loop filter. For the simulation of the loop filter in this thesis, the coherence time of the loop filter was chosen to be ten seconds. This corresponds to using ten data pulses to contribute to the error signal that drives the VCO.

The variance of the phase-error due to the intersymbol interference and additive Gaussian noise and conditioned on a particular data sequence is approximately

$$\sigma^2_{\Phi,\text{data}} = \frac{2B_L S_{n'}(0)}{(\overline{A^2})^2} \tag{22}$$

where B_L is the closed loop bandwidth and the power spectral density of the noise $S(f)$ is assumed constant over B_L (Ref 14:251 - 253). This assumes that the closed loop bandwidth B_L is much narrower than the bandlimited noise processes $n_1(t)$ and $n_2(t)$.

Computation of $\overline{A(t)^2}$. The time average of the input signal to the loop filter is

$$\overline{A^2(t)} = \frac{P}{T_L}\left[\int_0^{T_L} \sum_m p^2(t-mT)dt + \int_0^{T_L} \sum_m \sum_{\substack{n \\ m \neq n}} p(t-mT)p(t-nT)dt\right] \tag{23}$$

where the received signal power P is assumed constant over the coherence time of the loop.

From this equation, it can be seen that the net effect of ISI is to reduce the average dc signal that is applied to the VCO and to cause a random variation of the error

signal.

<u>Computation of $S_{n'}(0)$</u>. Applying the Fourier transform to Eq 21, the approximate power spectral density of the effective noise seen by the loop is

$$S_{n'}(0) = \frac{No}{2} R_A(0) + \left(\frac{No}{2}\right)^2 \tag{24}$$

where $R_A(0)$ is the total average power or the expression for $\overline{A^2(t)}$ that was developed in the preceding section.

The phase error variance conditioned on a particular data sequence and due to ISI and additive Gaussian noise is rewritten as

$$\sigma^2_{\Phi,\text{data}} = B_L \left[\left(\frac{No}{PI}\right)^2 \frac{1}{2} + \frac{No}{PI}\right]$$

$$\text{where } I = \left[\int_0^{T_L} \sum_m p^2(t-mT)dt + \int_0^{T_L} \sum_{\substack{m \\ m=n}} \sum_n p(t-mT)p(t-nT)dt\right] \tag{25}$$

Averaging this conditional variance over all of the possible combinations of data pulses in the coherence time of the loop,

$$\sigma^2_{\Phi} = \frac{1}{2^{[T_L/T_S]}} \sum_i^{2^{[T_L/T_S]}} \sigma^2_{\Phi,\text{data}_i} \tag{26}$$

where $[T_L/T_S]$ is the greatest integer value of the effective number of symbols used by the loop in making a phase estimate. For no ISI, I is just one and Eq 25 reduces to Eq 8.3.13 as given in Stiffler (Ref 14:247).

QCM Carrier Tracking Performance

For a received QCM signal plus noise as given in Equation 11, the inputs to the multiplier prior to the loop filter of Figure 3 are

$$Ae(t)\cos\Phi(t) + Ao(t)\sin\Phi(t) + n_1(t) \text{ (cosine leg)}$$

$$Ae(t)\sin\Phi(t) + Ao(t)\cos\Phi(t) + n_2(t) \text{ (sine leg)} \qquad (27)$$

where Ao(t) and Ae(t) are the summations of the odd and even interfering pulses. The output from the multiplier applied to the loop filter is

$$e(t) = \frac{(Ao^2(t) + Ae^2(t))}{2}\sin 2\Phi(t) + (Ae(t)\sin\Phi(t) + Ao(t)\cos\Phi(t))n_1(t) + (Ao(t)\sin\Phi(t) + Ae(t)\cos\Phi(t))n_2(t) + n_1(t)n_2(t) \qquad (28)$$

where $\Phi(t)$ and $n_1(t)$ and $n_2(t)$ are independent as before. Also, Ao(t) and Ae(t) are assumed to be independent since they are formed from a series of independent data pulses. The last three terms represent the total noise signal n'(t) which consists of additive Gaussian noise and intersymbol interference and has an autocorrelation of

$$R_{n'}(\tau) = R_{n_1}(\tau)[R_{Ao}(\tau) + R_{Ae}(\tau)] + R^2_{n_1}(\tau) \qquad (29)$$

The autocorrelations of Ao(t) and Ae(t) are easily obtained from the autocorrelation of A(t) for the BPSK case. The square of A(t) is written as the sum of the odd and

even terms squared, e.g. $A^2(t) = Ae^2(t) + Ao^2(t) + 2Ao(t)Ae(t)$. Therefore, the time average of the input signal to the loop filter, $\overline{Ao^2(t) + Ae^2(t)}$, is just $\overline{A^2(t)}$ from the BPSK case minus all of the terms of odd times even products in the second integral of Eq 23. Likewise, the total average power $[R_{Ae}(0) + R_{Ao}(0)]$ is $\overline{Ao^2(t) + Ae^2(t)}$.

<u>Tracking Penalty for QPSK versus BPSK/QCM with no ISI</u>

Although an expression was not obtained for the phase error variance of an N = 4 Costas loop, the energy penalty for tracking a quadrature versus a binary phase shift signal with no ISI can be used as a design consideration. The motivation for developing this expression is as follows: Since the error performance for QCM is very close to that of QPSK for the same data rates and transmitter power, perhaps QCM could be used to an advantage where phase instabilities are a problem. The bandwidth of a QCM carrier tracking loop can be increased so as to obtain a faster response time to these phase changes than can be obtained from QPSK for a given transmitter power. Alternately stated, when the maximum phase error and response time of a system is specified, what is the increase in Eb/No that must be applied to a QPSK system so it has the same tracking characteristics as a QCM system?

Equating the expressions for phase error variance for BPSK (also QCM) and QPSK under no ISI yields

$$T_S B_L[1/(Z-a) + 1/2(Z-a)^2] = T'_S B'_L[1/Z + 9/2\,Z^2 + 6/Z^3 + 3/2\,Z^4] \tag{30}$$

where Z is the bit signal-energy-to-noise ratio for QPSK, T_S and T'_S are the symbol intervals, and B_L and B'_L are the bandwidths of the closed loops (Ref 14: Eq 8.3.13). For a fair comparison of the two systems the information rates are the same ($T'_S = T_S/2$), and the responses of the tracking loops are the same ($B'_L = B_L$).

Fixing the right hand side of Eq 30 at some signal-energy-to-noise ratio Zo and then making the change of variable Z - a = X produces a quadratic equation in X.

$$A(Zo)\,X^2 - X - \frac{1}{2} = 0 \qquad (31)$$

where A(Zo) is the right hand side of Eq 30 in brackets evaluated at Zo. Because the energy signals cannot be negative and the discriminant is always greater than zero, the signal-energy-to-noise ratio of the QCM case is

$$X = \frac{1 + \sqrt{1 + 2A(Zo)}}{2A(Zo)}$$

for the same phase error variance, response to phase instabilities, and information rate as the QPSK case.

III. Numerical Results

In Chapter II, equations are given for the conditional probabilities of error for BPSK, QCM, and QPSK in the presence of intersymbol interference. Also given are the average phase error variances for BPSK and QCM, and the energy penalty for tracking a quadrature versus a binary modulated signal. In this chapter, numerical results from these equations are obtained in order to compare QCM, BPSK, and QPSK systems. First, the philosophy for including only those interfering pulses within a certain power threshold is discussed, and a comparison with Jones's results is shown. The conditional error probabilities are then compared for BPSK, QCM and QPSK. Following that, the phase error variances for BPSK and QCM are examined. Finally the energy penalty for tracking a QPSK signal versus a QCM or BPSK signal is presented. The overall conclusion is that QCM performs better than BPSK and is only slightly inferior in data detection performance to QPSK.

Truncation of Data Sequence

A major problem in this thesis was how many interfering pulses should be included to obtain sufficiently accurate numerical results. Jones has stated that, except for low BT products, satisfactory results can be obtained in evaluating error probabilities by considering only the most adjacent interferer from the past data bit (Ref 11:126). However, he did not state at what BT product this assumption

becomes invalid. The number of past bits (KP) used for the binary modulation schemes for this thesis was chosen to be KP = 9 - KF, where the future bits (KF) are determined from the group delay in Table I, Chapter II. With this algorithm, the power levels of all pulses outside of the truncated data sequence are at least 20 dB below the power of the current datum pulse for a BT of 0.5 (the worst case of ISI). While this results in including terms below the 20 dB threshold for higher BT products, their inclusion should only serve to increase the accuracy of those results.

The power threshold of 20 dB was verified by comparing the conditional probability of error for BPSK for two adjacent interfering pulses and for the nine interfering pulses from Table II. These results are shown in Table III for a bit signal-energy-to-noise ratio of 10 dB. This comparison shows the necessity for including more than two adjacent bits as the BT product approaches 0.5 to obtain more than one significant figure of accuracy. The -20 dB power threshold is assumed to be adequate with the following reasoning: The two adjacent bits for a BT = 1.0 correspond to including all pulses within a power threshold of only -15.5 dB. Increasing the number of bits to nine for a BT = 1.0 results in considering all pulses within a threshold of -42 dB; however, this only changes the fourth significant digit in the probability of error results. Thus, a power threshold of -20 dB for the worst case (BT = 0.5) was arbitrarily chosen to lie between these values, and is expected to

Table III

BPSK Conditional Probability of Error

(Phase Error = 0^{o})

BT	$P(e\|\Phi)$ Two Adjacent Pulses KP = KF = 1	Nine Pulses KP + KF = 9	KF	KP
0.5	1.6730(-3)	2.0701(-3)	2	7
1.0	5.1155(-5)	5.1181(-5)	1	8
1.5	2.1854(-5)	2.1943(-5)	1	8

Note: The negative integer in parentheses following each entry represents the power of ten by which the entry should be multiplied.

produce probability of error results that are accurate in the third significant digit. Similar reasoning was used in the QPSK case; however, the threshold was arbitrarily established at -30 dB.

The BPSK case for no phase error is compared to Jones's Fig. 6. This comparison is shown in Table IV as an increase in the signal energy (δEb) from the ideal case of no ISI (BT = ∞) required to maintain a bit probability of error of 10^{-6} with perfect coherent detection assumed. It should be noted that Jones defines his BT on the basis of a two-sided bandwidth; therefore, his BT of 2.0 corresponds to a BT of 1.0 as used in this thesis. This comparison was important

for three reasons. First, the correlation of the two methods served to verify that the programs in this thesis were operating correctly. Second, the increasing difference between the two methods as the BT is decreased verified Jones's conclusion that more than one adjacent bit is required for low BT products. Finally, for BT levels of 1.0 or less, more than one adjacent bit should be included to obtain sufficiently accurate results.

Table IV

Signal Energy Required to Maintain $P(e|\Phi) = 10^{-6}$ for BPSK in Presence of ISI (Phase Error = 0°)

BT	δEb Jones's Method (dB)	δEb Thesis Method (dB)
0.5	5.4*	4.8
1.0	1.1*	1.3
1.5	1.0*	0.9

*Interpolated values for a six-pole filter (Ref 11:126 Fig. 6).

Conditional Probability of Error

The conditional error probabilities of BPSK, QCM, and QPSK averaged over the truncated data stream and conditioned on phase errors of 0°, 10°, and 20° are compared. These

conditional probabilities are also examined relative to the ideal signal case (no intersymbol interference and perfect coherent detection).

<u>BPSK versus QCM</u>. In Figures 7, 8, and 9 the conditional error probabilities of the BPSK and QCM signals with phase errors of 0°, 10°, and 20° are shown. These probability of error plots show the improvement over normal BPSK by using QCM. The degrading effects of an increasing phase error are apparent when these figures are compared to each other. Tables V, VI, and VII compare BPSK and QCM for selected signal-energy-to-noise ratios. The tables show that although QCM has a lower probability of error than BPSK, it is more sensitive to a change in phase error than BPSK.

Nielsen compared these two modulation techniques with an improvement factor defined as the Eb/No (dB) a QCM signal requires to obtain an error probability of 10^{-5} minus the Eb/No (dB) a BPSK signal needs to produce the same probability of error (Ref 3:29, Table VI). He found an extremely high improvement factor (greater than 25 dB) with a BT of 0.5. This author feels these are a result of the incorrect group delay and the missing term in Nielsen's Eq 15.

For this thesis, an improvement factor, β, is defined as the difference in Eb/No (dB) for two signalling schemes in order to produce the same specified probability of error. A power penalty is defined as the additional power (dB) beyond the ideal case ($BT = \infty$) required to maintain the same specified probability of error. In Table VIII, this im-

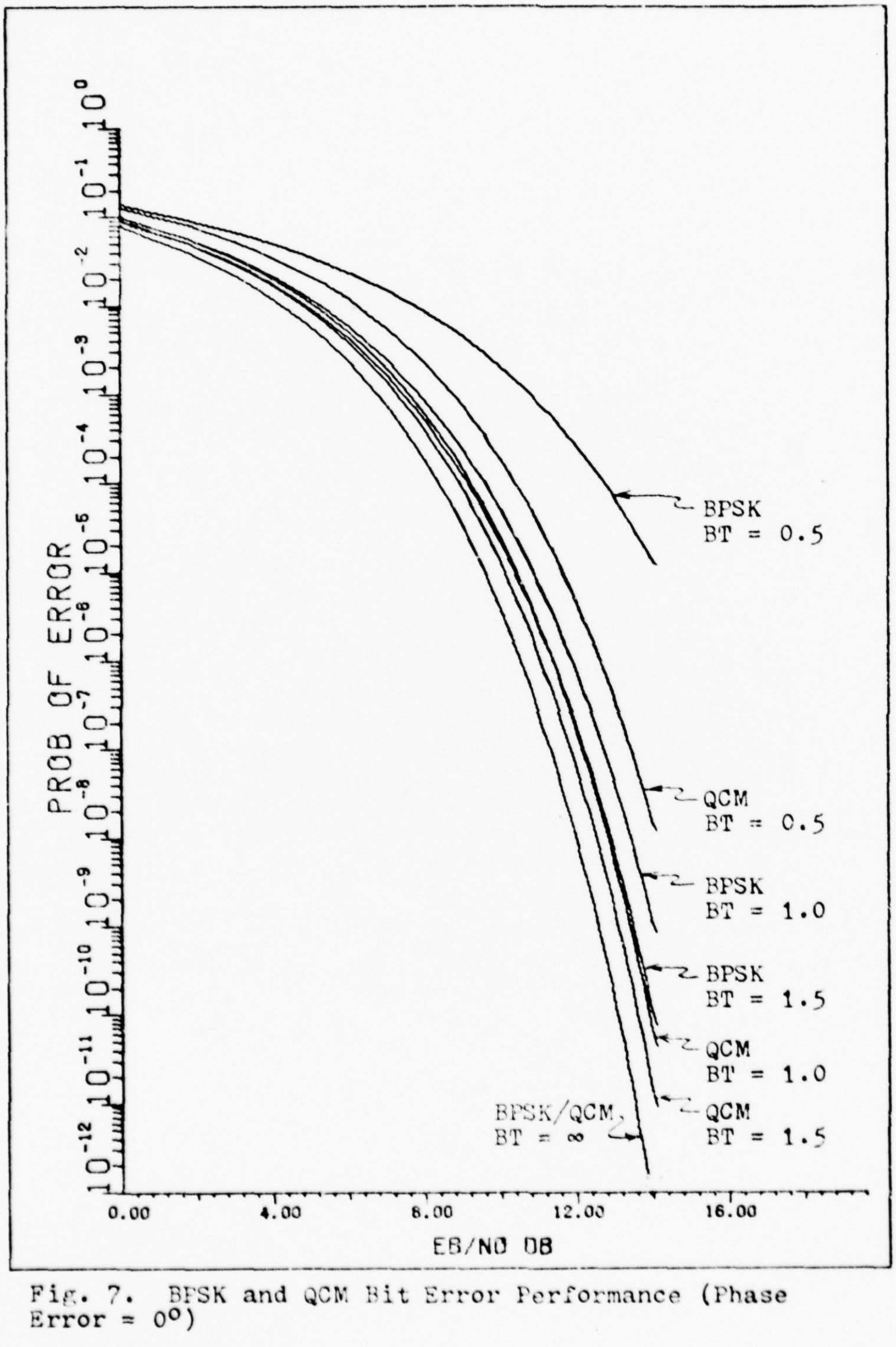

Fig. 7. BPSK and QCM Bit Error Performance (Phase Error = 0°)

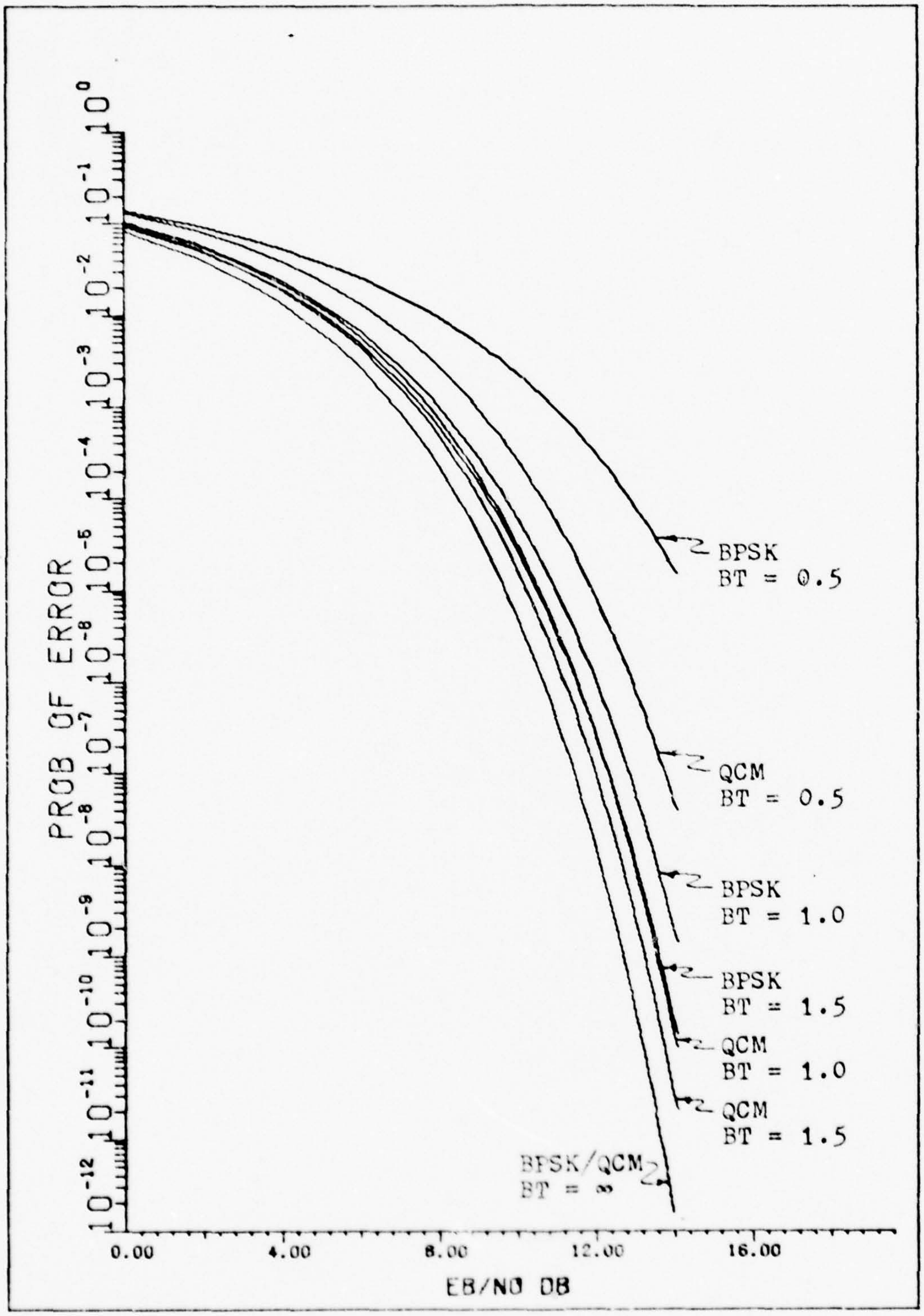

Fig. 8. BPSK and QCM Bit Error Performance (Phase Error = 10°)

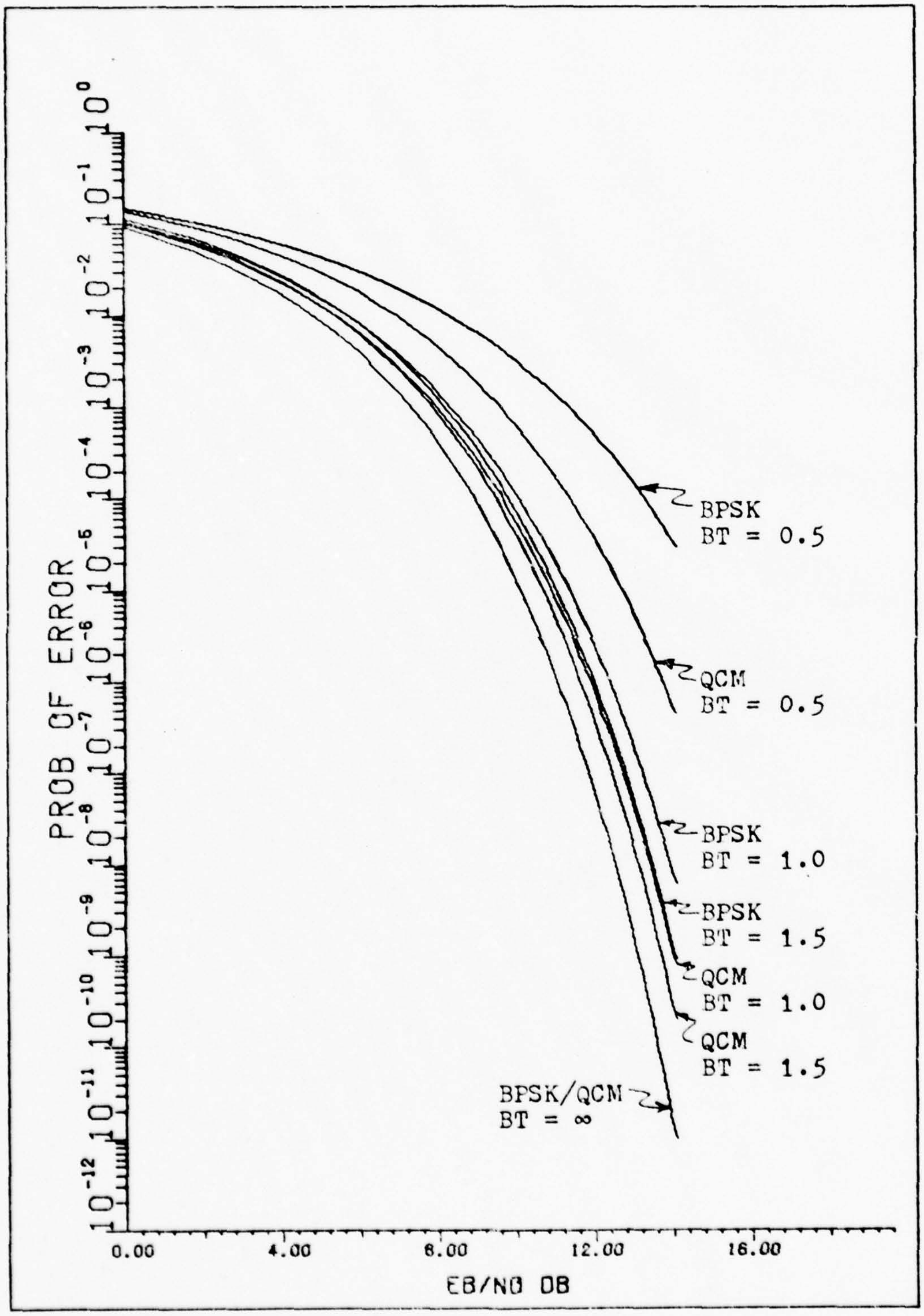

Fig. 9. BPSK and QCM Bit Error Performance (Phase Error = 20°)

Table V

Conditional Probability of Error

For a BT of 0.5

Eb/No dB	Phase Error, degrees	P(e|Φ) BPSK	QCM
0	0	0.1375	0.1280
0	10	0.1409	0.1319
0	20	0.1514	0.1440
6	0	0.2369(-1)	0.1181(-1)
6	10	0.2508(-1)	0.1326(-1)
6	20	0.2968(-1)	0.1834(-1)
10	0	0.2070(-2)	0.1907(-3)
10	10	0.2316(-2)	0.2700(-3)
10	20	0.3210(-2)	0.6634(-3)
12.5	0	0.1281(-3)	0.1156(-5)
12.5	10	0.1532(-3)	0.2457(-5)
12.5	20	0.2585(-3)	0.1379(-4)

Note: The negative integer in parenthesis following each entry in the table represents the power of ten by which the entry should be multiplied.

Table VI

Conditional Probability of Error

For a BT of 1.0

Eb/No dB	Phase Error degrees	$P(e\|\Phi)$ BPSK	$P(e\|\Phi)$ QCM
0	0	0.1008	0.9960(-1)
0	10	0.1042	0.1030
0	20	0.1149	0.1139
6	0	0.5935(-2)	0.5119(-2)
6	10	0.6585(-2)	0.5751(-2)
6	20	0.8906(-2)	0.8044(-2)
10	0	0.5118(-4)	0.2456(-4)
10	10	0.6418(-4)	0.3280(-4)
10	20	0.1238(-3)	0.7473(-4)
12.5	0	0.1571(-6)	0.2566(-7)
12.5	10	0.2306(-6)	0.4426(-7)
12.5	20	0.6994(-6)	0.2038(-6)

Table VII

Conditional Probability of Error

For a BT of 1.5

Eb/No dB	Phase Error degrees	P(e|Φ) BPSK	QCM
0	0	0.9239(-1)	0.9163(-1)
0	10	0.9574(-1)	0.9502(-1)
0	20	0.1062	0.1056
6	0	0.4320	0.3890(-2)
6	10	0.4840(-2)	0.4397(-2)
6	20	0.6731(-2)	0.6264(-2)
10	0	0.2194(-4)	0.1290(-4)
10	10	0.2830(-4)	0.1740(-4)
10	20	0.5914(-4)	0.4102(-4)
12.5	0	0.3091(-7)	0.8284(-8)
12.5	10	0.4791(-7)	0.1440(-7)
12.5	20	0.1699(-6)	0.6893(-7)

Table VIII

Conditional Performance

For $P(e|\Phi)$ of 10^{-5}

BT	Phase Error degrees	Eb/No, dB BPSK	Eb/No, dB QCM	β, dB	Power penalty QCM, dB
∞	0	9.54	9.54	0.0	0.0
∞	10	9.80	9.80	0.0	0.0
∞	20	10.10	10.10	0.0	0.0
1.5	0	10.40	10.10	0.30	0.56
1.5	10	10.50	10.20	0.30	0.40
1.5	20	10.90	10.70	0.20	0.60
1.0	0	10.80	10.41	0.39	0.87
1.0	10	10.97	10.60	0.37	0.80
1.0	20	11.35	11.00	0.35	0.90
0.5	0	14.30	11.61	2.69	2.07
0.5	10	14.36	11.90	2.46	2.10
0.5	20	14.46	12.67	1.79	2.57

provement factor, β, is shown for an error probability of 10^{-5}; also shown is the power penalty of QCM for the ideal case. This comparison illustrates that QCM has little value over normal BPSK for BT products of 1.0 or larger, and clearly shows the convergence of QCM towards BPSK as the phase error increases towards $\pi/4$ radians.

QPSK versus QCM. In Figures 10, 11, 12 the conditional probabilities of symbol error for QPSK with phase errors of 0^{o}, 10^{o}, and 20^{o} are shown. The BT products for the QPSK plots are chosen to correspond to the same information rate for the QCM plots. Tables IX and X compare QPSK and QCM bit error probabilities for selected signal-energy-to-noise ratios for the QCM/QPSK BT pairs of 0.5/1.0 and 1.0/2.0. These comparisons of QPSK and QCM illustrate the almost equal performance that can be obtained from QCM relative to QPSK.

In Figure 13 the conditional bit error probabilities are plotted for QCM/QPSK signal pairs of (0.5/1.0), (0.75/1.5), and (1.0/2.0) with coherent detection assumed. This figure shows that, although QPSK is better, QCM may perform with about the same probability of error with a BT of 0.75. Table XI gives the improvement factor for QCM versus QPSK for selected bit probabilities of error and a BT pair of 0.75/1.5. Here, QCM has at most an Eb/No penalty of 0.26 dB, at a bit probability of error of 10^{-3}, when compared to QPSK.

The almost equal performance between QCM and QPSK suggest that QCM could be used to an advantage over QPSK where car-

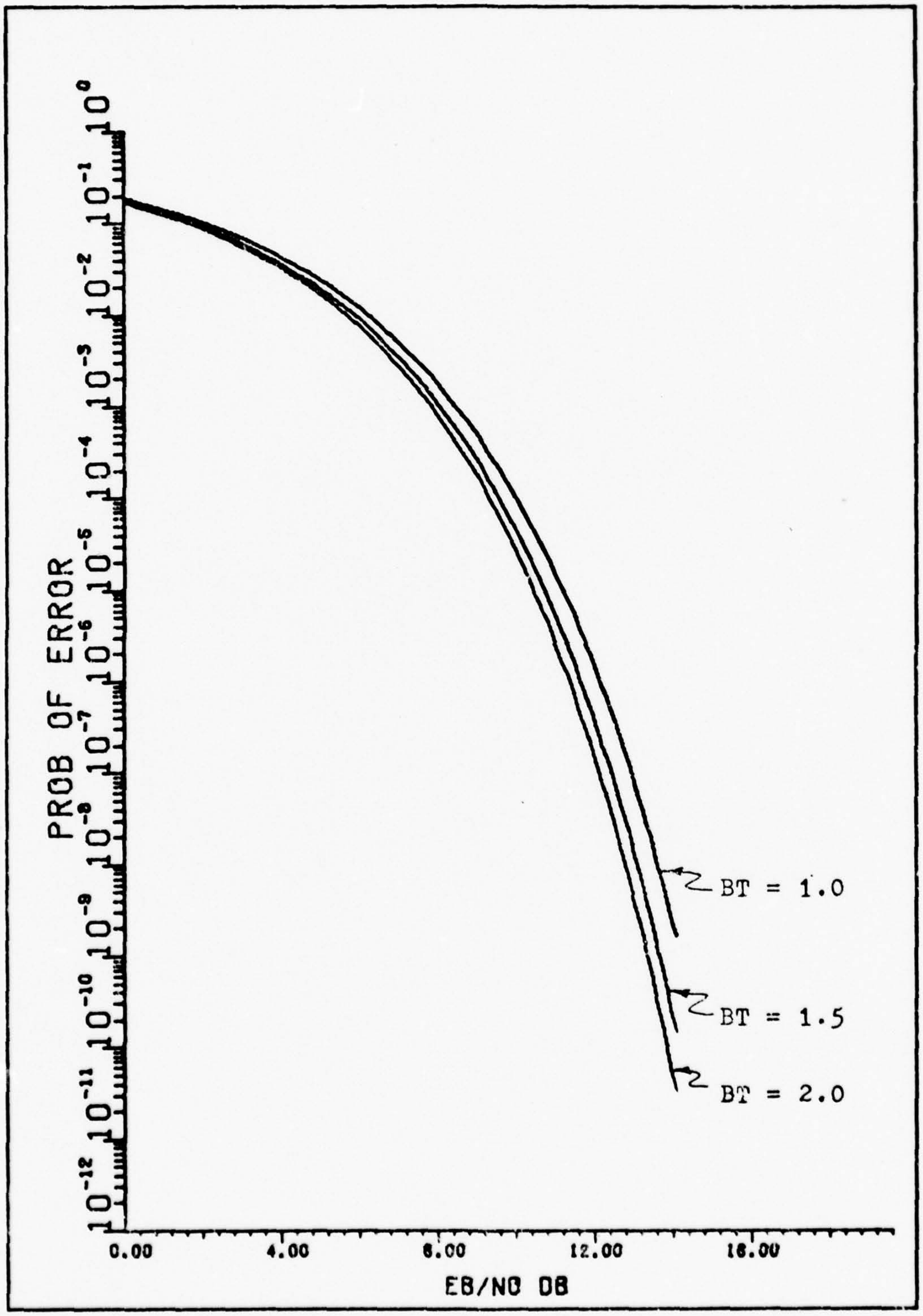

Fig. 10. QPSK Symbol Error Performance (Phase Error = 0^{o})

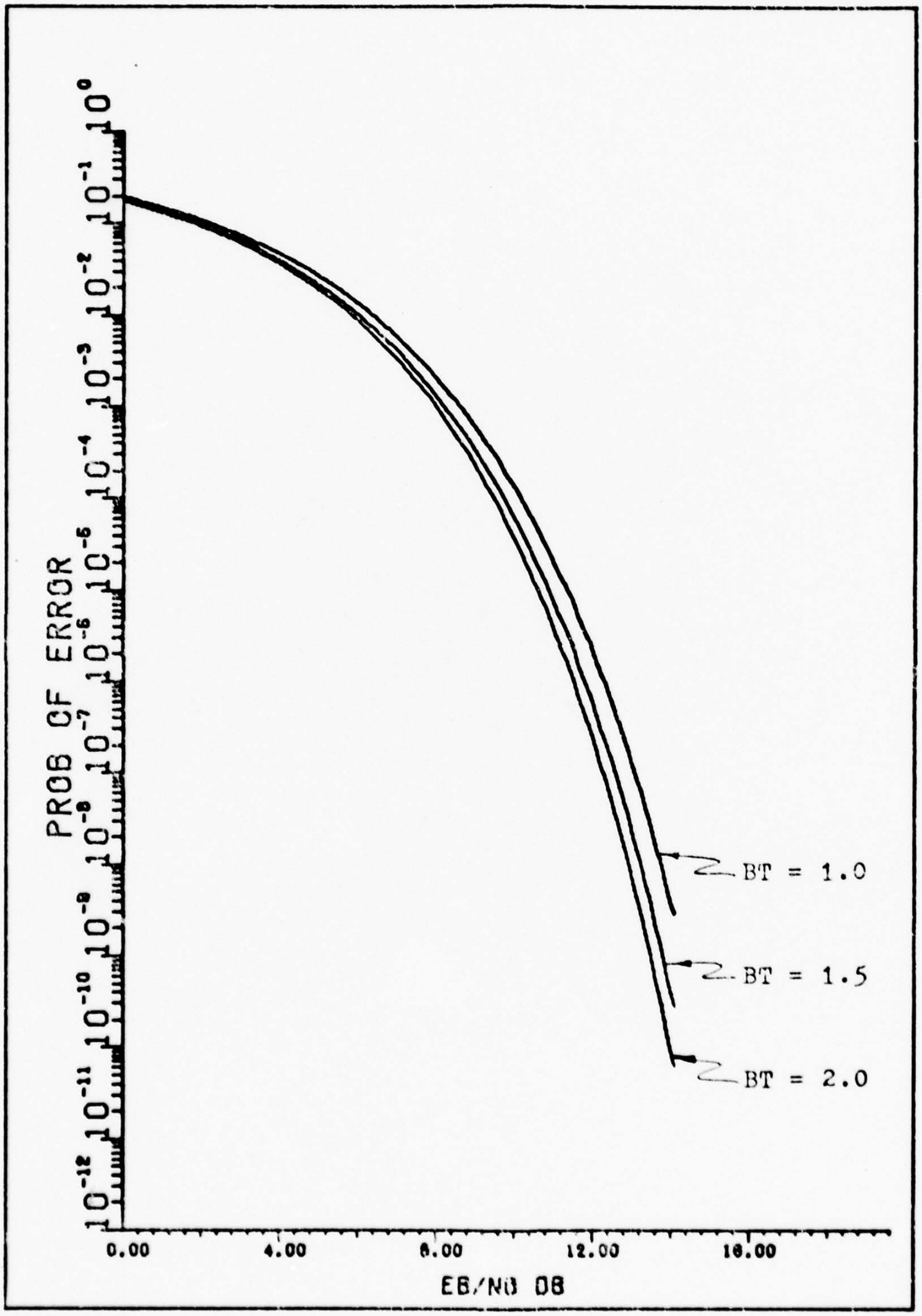

Fig. 11. QPSK Symbol Error Performance (Phase Error =10°)

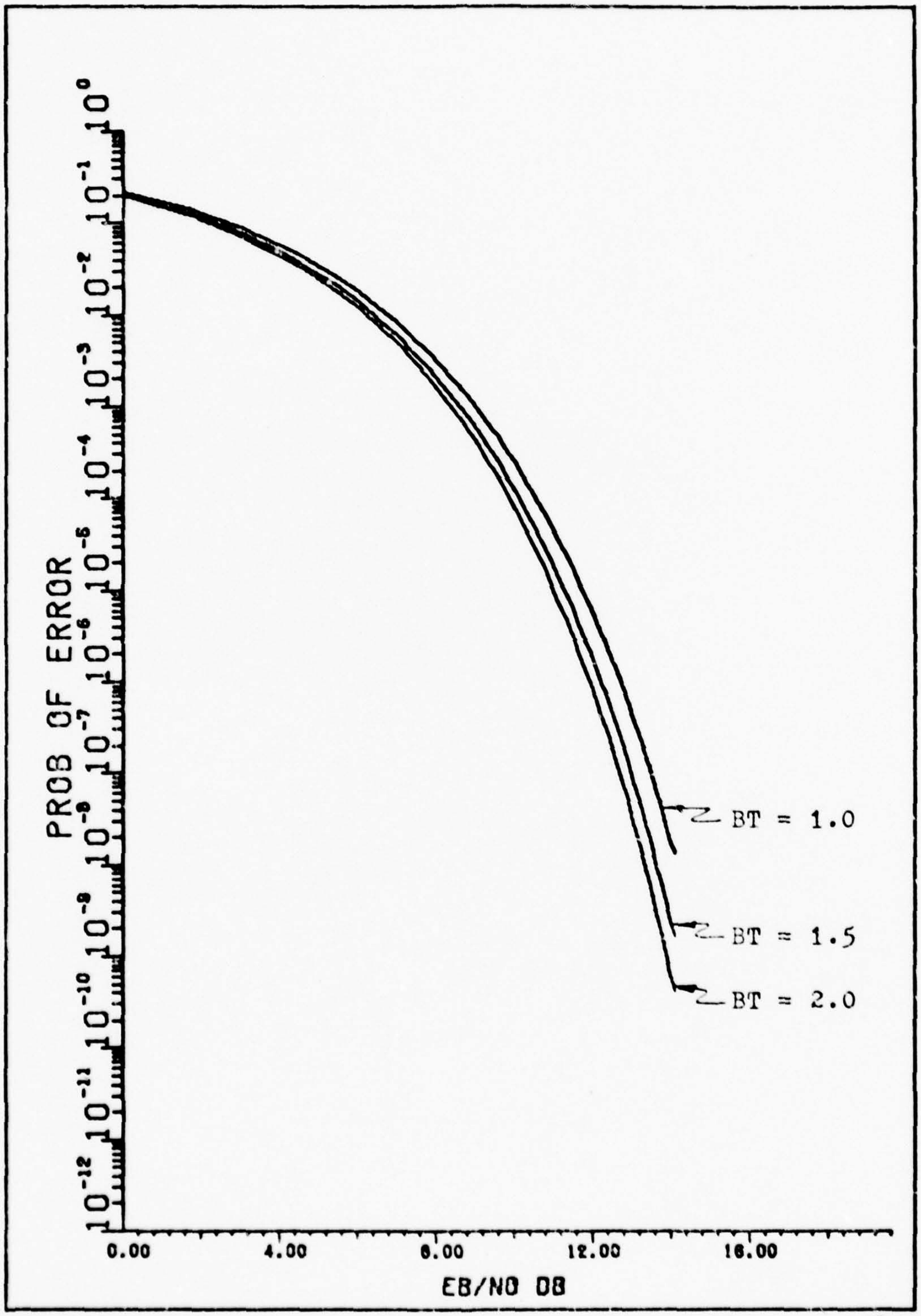

Fig. 12. QPSK Symbol Error Performance (Phase Error = 20°)

Table IX

Conditional Probability of Error

For a QCM/QPSK BT of 0.5/1.0

Eb/No dB	Phase Error degrees	P(e| Φ) QPSK	QCM
0	0	0.9571(-1)	0.1280
0	10	0.9878(-1)	0.1319
0	20	0.1083	0.1440
6	0	0.5918(-2)	0.1181(-1)
6	10	0.6563(-2)	0.1326(-1)
6	20	0.8866(-2)	0.1834(-1)
10	0	0.5118(-4)	0.1907(-3)
10	10	0.6418(-4)	0.2700(-3)
10	20	0.1237(-3)	0.6634(-3)
12.5	0	0.1571(-6)	0.1156(-5)
12.5	10	0.2305(-6)	0.2457(-5)
12.5	20	0.6993(-6)	0.1379(-4)

Table X

Conditional Probability of Error

For a QCM/QPSK BT of 1.0/2.0

Eb/No dB	Phase Error degrees	P(e|Φ) QPSK	QCM
0	0	0.8486(-1)	0.9960(-1)
0	10	0.8789(-1)	0.1030
0	20	0.9731(-1)	0.1139
6	0	0.3631(-2)	0.5119(-2)
6	10	0.4093(-2)	0.5751(-2)
6	20	0.5787(-2)	0.8044(-2)
10	0	0.1283(-4)	0.2456(-4)
10	10	0.1687(-4)	0.3280(-4)
10	20	0.3732(-4)	0.7473(-4)
12.5	0	0.1065(-7)	0.2566(-7)
12.5	10	0.1709(-7)	0.4426(-7)
12.5	20	0.6711(-7)	0.2038(-6)

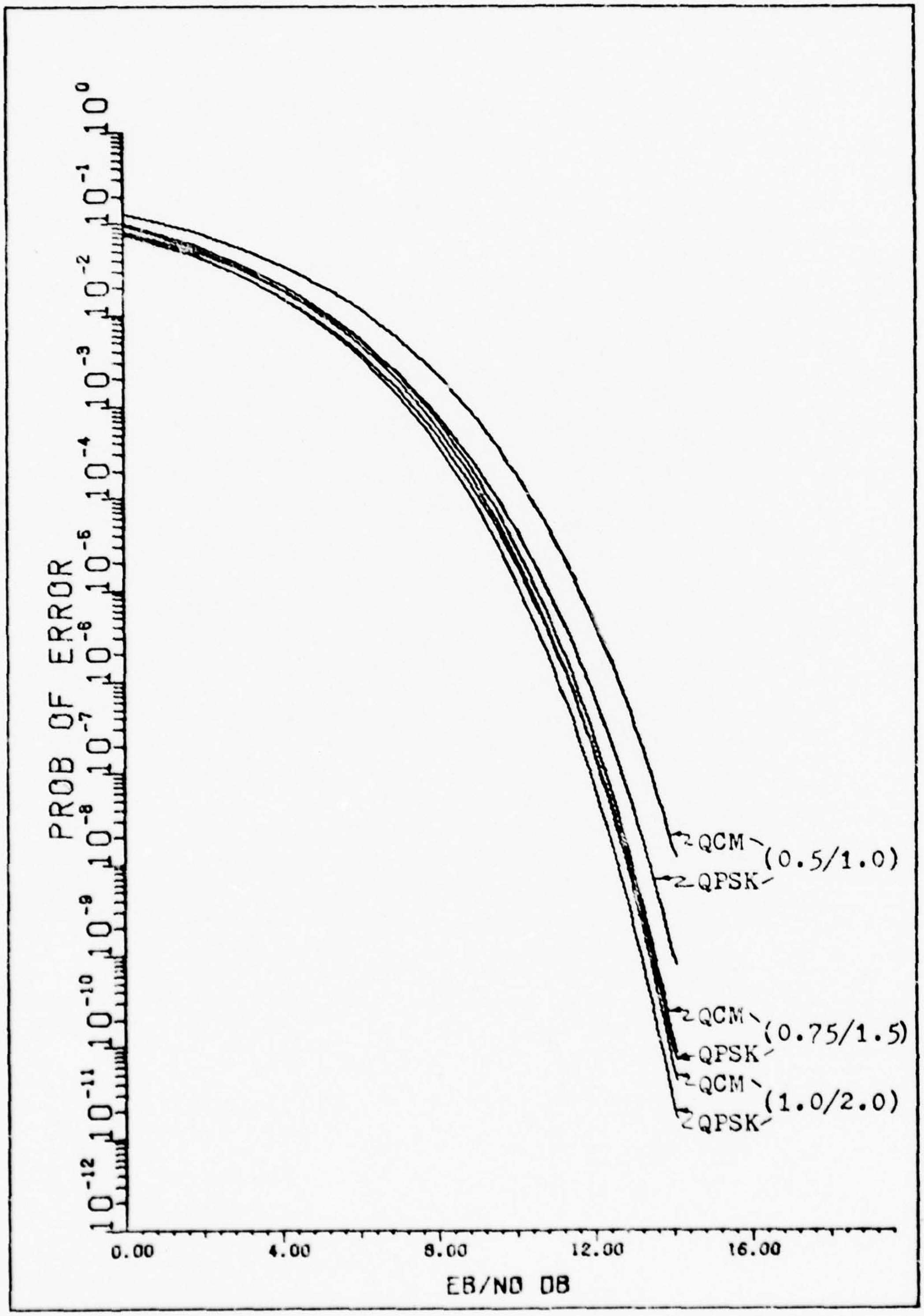

Fig. 13. QPSK/QCM Bit Error Performance (Gray Code Assumed; Phase Error = 0°)

Error = 0^{o})

Table XI

Conditional Bit Error Performance For

QCM/QPSK with a BT of 0.75/1.5

(Phase Error = 0^{o})

$P(e\|\Phi)$	Eb/No, dB		β, dB	Power Penalty
	QPSK	QCM		QPSK, dB
0.1(-1)	4.59	4.77	-0.16	0.57*
0.1(-2)	7.49	7.75	-0.26	0.95*
0.1(-3)	9.15	9.37	-0.21	0.70*
0.1(-5)	11.30	11.46	-0.16	-

*Ideal bit probability of error for QPSK was obtained from Lindsey and Simon (Ref 16:232, Table 5-3).

rier tracking instabilities are a problem. As an example, in a low signal-to-noise environment where transreceiver instabilities, Doppler phase shifts, and random variations in the modulating signal cause inherent difficulties in tracking the carrier of a quadrature modulated signal, the carrier of a binary modulated signal can still be tracked. This will be discussed further when the Eb/No penalty for tracking a QPSK signal versus a QCM signal is examined.

Phase Error Variance

The average phase error variance is obtained by a numerical evaluation of Eq 24 for BPSK and QCM in the presence of ISI. The phase error variance is plotted as a function of the signal-energy-to-noise ratio and filter BT products times a closed-loop bandwidth in Figures 14 and 15. These plots also show the phase error variance for no ISI ($BT = \infty$). For data rates corresponding to BT products of 1.0 or higher, the phase error variance is approximately the same as that for no ISI. For a BT of 0.5 with signal-energy-to-noise ratios of 6 dB or more, the phase error variance is increased by at most 0.18 Rad/Hz over the ideal case of no ISI. The 6 dB signal to noise ratio was arbitrarily chosen to correspond to a probability of error of 0.05 for BPSK operating with a phase error of 20°. This is expected to be the worst data performance that could be tolerated with direct data detection (no encoding).

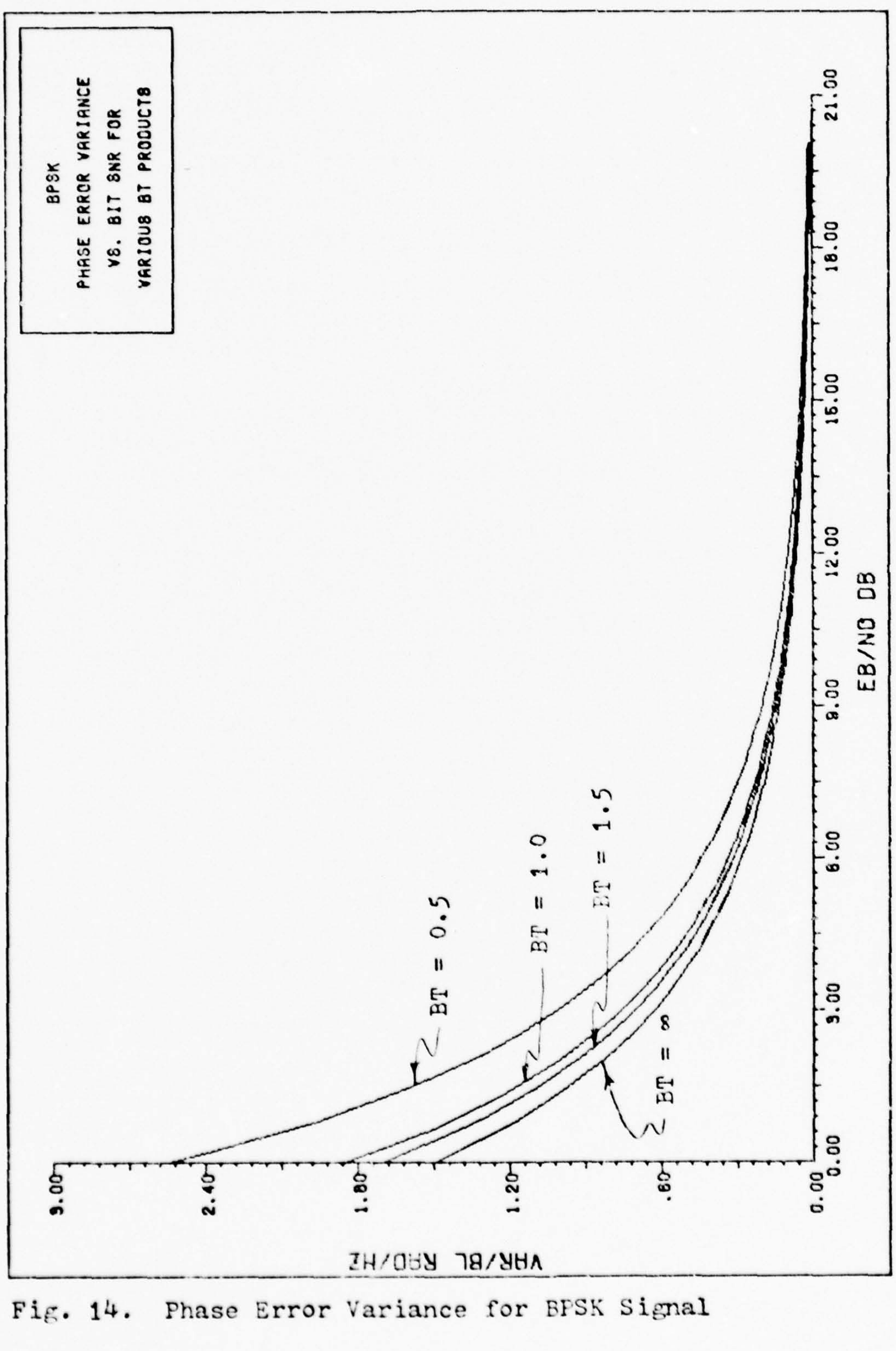

Fig. 14. Phase Error Variance for BPSK Signal

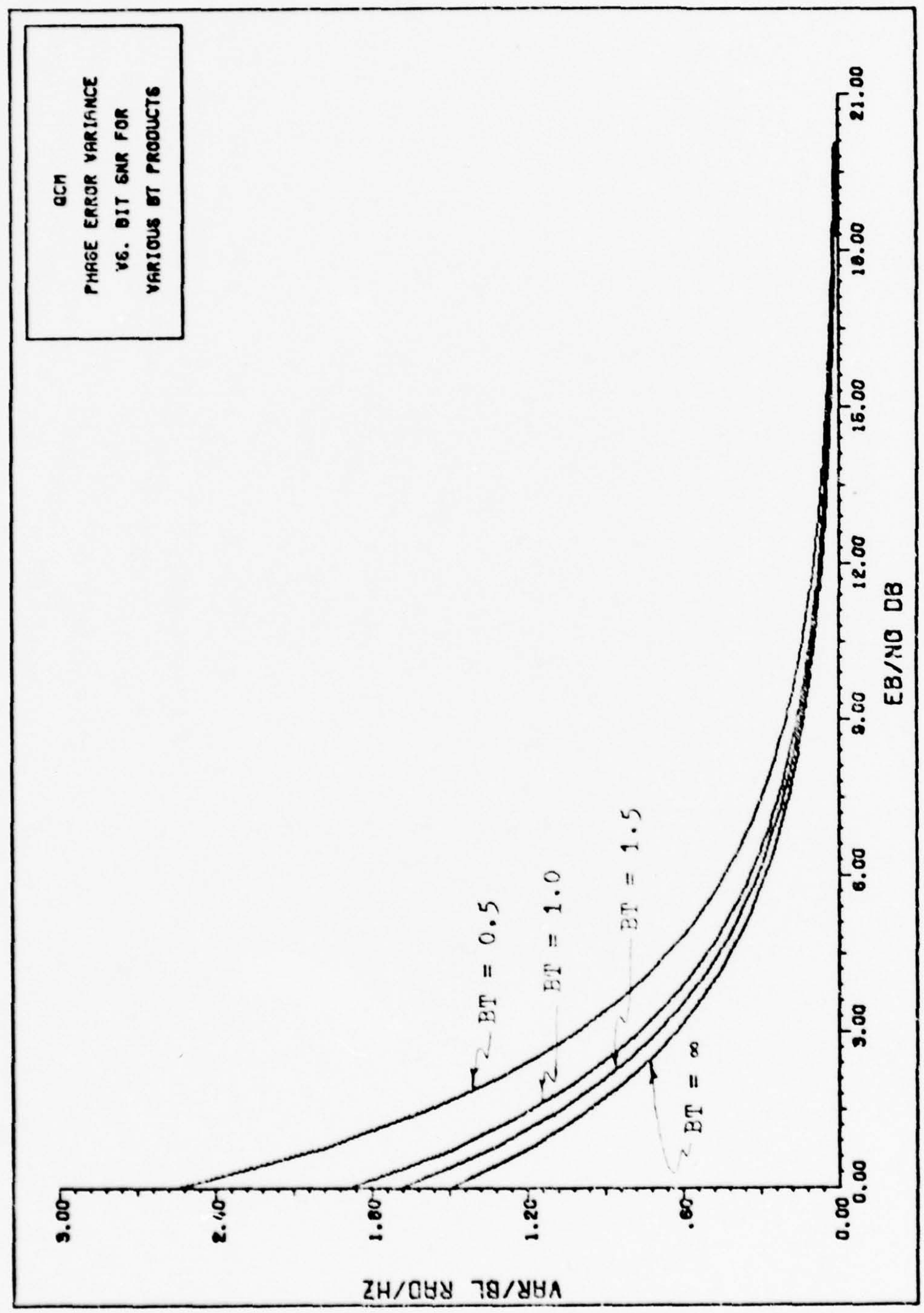

Fig. 15. Phase Error Variance for QCM Signal

QPSK Tracking Penalty

The bit signal energy penalty for tracking a quadrature modulated signal versus a binary signal with no ISI and the same phase error variance and loop response is illustrated in Figure 16. The energy penalty is defined as the additional bit signal-energy-to-noise ratio Eb/No in dB that a QPSK system would require as a function of the BPSK Eb/No. While this energy penalty was obtained under no ISI conditions, it is assumed that it can be used as a rough approximation for the tracking penalty QPSK would suffer over QCM under ISI conditions.

In order to best understand the importance of this energy penalty consider the following: In the design of any carrier tracking loop, the closed-loop bandwidth is made as narrow as possible so as to minimize the effects of the noise process on the phase error, but still wide enough so the loop will respond to the various phase instabilities (Ref 15:133-134). In this design process, it is tacitly assumed that the carrier tracking portion of the receiver has a sufficient front-end signal-to-noise ratio to maintain the loop in a locked condition. For a decreased input signal to noise ratio, the closed-loop bandwidth can be decreased, but only at the expense of reducing the response of the filter to the phase variations. In general, linear loop analysis predicts that this trade-off between the noise and phase processes becomes more critical as the number of signalling phases increase (Ref 14:247). In some situations, a low received signal-to-noise ratio (SNR) combined with excessive

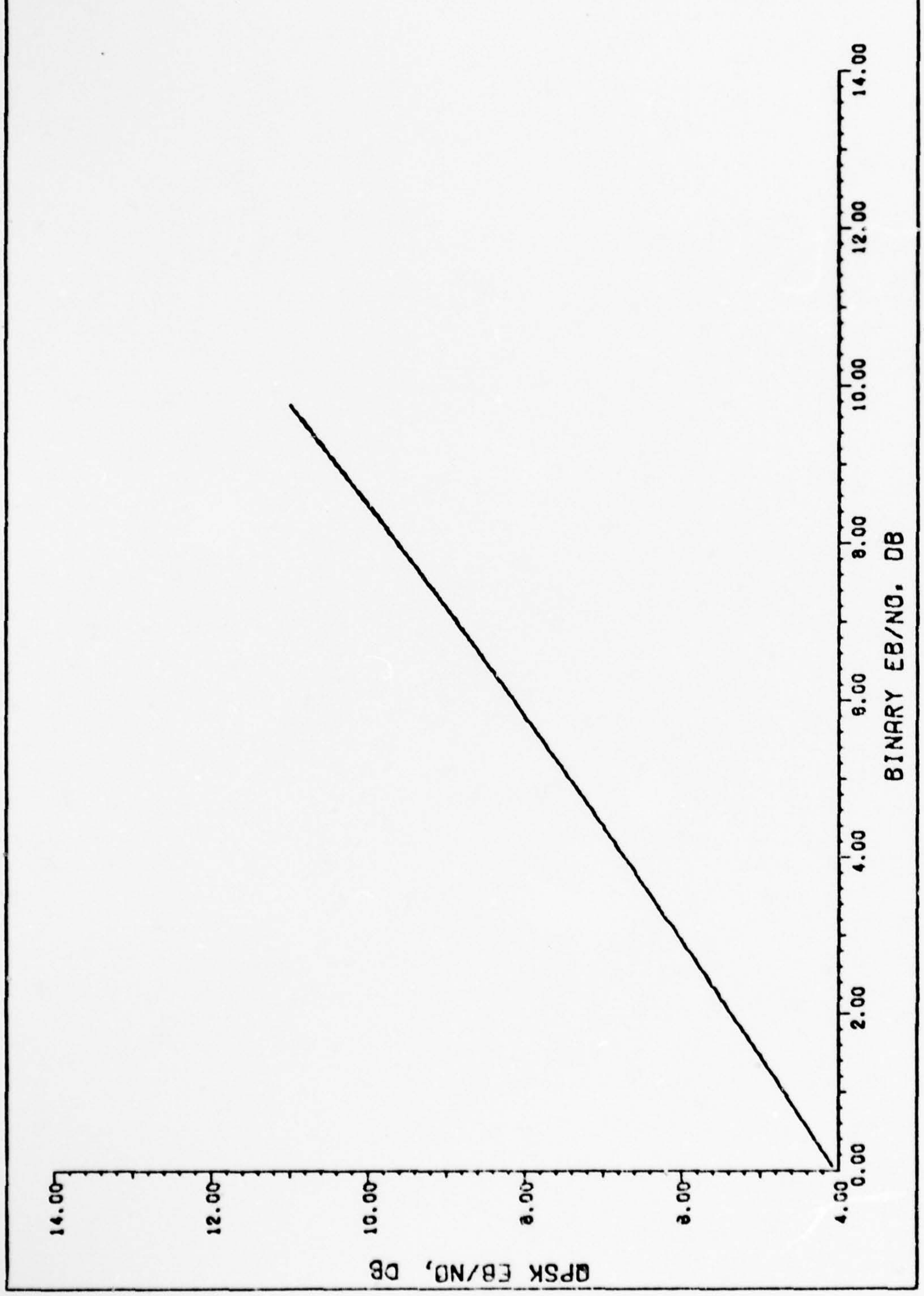

Fig. 16. QPSK versus Binary Eb/No for Equal Phase Error Variance and Loop Response and Information Rates

random phase processes will prevent proper loop tracking. These random phase processes are the transreceiver instabilities, Doppler phase shifts, and variations in the phase modulation (Ref 15: Eq 4-8).

When improper loop tracking occurs for QPSK, an alternative signalling method such as BPSK can sometimes still be tracked. As shown in Figure 16, a BPSK signal with an Eb/No of 5.0 dB corresponds to a QPSK signal with an Eb/No of 7.4 dB for the same information rate and loop tracking characteristics. Suppose, for example, a QPSK system was plagued by phase instabilities such that it fell out of lock with an Eb/No of 7.3 dB. A binary modulated system could be switched in at this point and still continue to operate until nearly 5.0 dB before it also fell out of lock. This procedure, i.e. switching in BPSK as a back-up to QPSK, has been proposed for DSCS-III. Naturally, because of the lower Eb/No, the probability of error will increase.

Because QCM has a superior performance to BPSK and because QCM is also a binary modulated signal it should be considered as an alternative back-up signalling scheme for QPSK. Clearly, only a slight improvement could be gained by using QCM versus BPSK as a back-up scheme where BT products of 1.0 or higher are used. However, for data rates corresponding to a BT = 0.5 up to a 2.7 dB gain in data performance could be realized over the BPSK system. Obviously, no strong conclusions can be made concerning QCM as a back-up system for QPSK until the tracking penalty for

a QPSK system is obtained in the presence of ISI.

IV. Conclusions and Recommendations

Conclusions

QCM gives better performance than BPSK when used in a communication system limited by intersymbol interference. For data rates corresponding to BT products of 1.0 or more, the actual gain over BPSK is negligible. However, for an increased data rate corresponding to a BT of 0.5, an improvement of 2.69 dB is obtained for an error probability of 10^{-5}. Thus, a change from BPSK to QCM could allow one to maintain the same probability of error at almost double the data rate.

QCM was found to be inferior to QPSK when compared on the basis of equal bit information rates. However, the difference between QCM and QPSK is small. For example, QCM suffered at most a 0.8 dB penalty when compared to QPSK for a BT pair of 0.5/1.0 and an error probability of 10^{-5}. And for a BT pair of 0.75/1.5 the performance of QCM was almost equal to that of QPSK. This almost equal performance suggests that QCM, and not BPSK, should be considered as an alternate signalling scheme if phase tracking cannot be maintained for QPSK.

QCM introduces no problems in the carrier tracking capability of a Costas loop, and, in fact, the average phase error variance of a Costas loop was found to be essentially equal for BPSK and QCM for the BT products considered in this thesis. For data rates corresponding to BT products

of 1.0 or more, the phase error variance is close to the ideal wideband case ($BT = \infty$). For a BT of 0.5, the phase error variance is increased from the ideal case by at most 0.18 rad/Hz for received signal-energy-to-noise ratios of 6 dB or more.

Recommendations

Other aspects of QCM versus BPSK and QPSK should be investigated. A comparison of QPSK, BPSK, and QCM should be made assuming that the timing information is in error. This timing error could possibly be modeled as a random variation applied to the group delay, τ.

Another area of investigation is a comparison of the three modulation schemes with an additional method of reducing intersymbol interference. As an example, does the application of equilization to the three signalling schemes cause any reversal of the hierarchy of performance that was obtained in this thesis?

A third area of consideration is a comparison of the phase tracking characteristics of QCM versus QPSK in the presence of intersymbol interference. Although this thesis has shown the Eb/No penalty that a fourth order loop suffers over the binary modulated case under no ISI, it is not known if the effects of ISI would change these results.

Bibliography

1. Messerschmitt, D.G. "A Geometric Theory of Intersymbol Interference." The Bell System Technical Journal, 49: 1483-1539 (November 1973).

2. Kullstam, Per A. "Quadrature Clock Modulation as Applied to Spread Spectrum Communications." An unpublished Computer Science Corporation Interoffice Correspondence dated September 19, 1973. Computer Sciences Corporation, Falls Church, Virginia.

3. Nielsen, Wade L. "Quadrature Clock Modulation and Binary Phase Shift Keying Signalling in the Presence of Intersymbol Interference." Masters thesis dated December 1976. United States Air Force Institute of Technology, Wright-Patterson Air Force Base, Ohio.

4. Ziemer, R.E. and W.H. Tranter. Systems, Modulation, and Noise. Boston, Mass.: Houghton Mifflin Company, 1976.

5. Chapuran, Robert C. Telephone interview. Defense Communication Engineering Center/R420, 1860 Wiehle Ave, Reston, Virginia, September 15, 1977.

6. Ho, E.Y. and Y.S. Yen. "A New Approach to Evaluating the Error Probability in the Presence of Intersymbol Interference and Additive Gaussian Noise." The Bell System Technical Journal, 49:2249-2265 (November 1970).

7. Prabhu, Vasant K. "Performance of Coherent Phase-Shift-keyed Systems With Intersymbol Interference." IEEE Transactions on Information Theory, IT-17 4:418-431 (July 1971).

8. Prabhu, Vasant K. "Error Probability Performance of M-ary CPSK Systems with Intersymbol Interference." IEEE Transactions on Communication Technology, COM-21 2:97-109 (February 1973).

9. Shimbo, O., R.J. Fang, and M. Celebiler. "Performance of M-ary PSK Systems in Gaussian Noise and Intersymbol Interference." IEEE Transactions on Information Theory, IT-19 1:44-58 (January 1973).

10. Rice, S.O. "Distribution of Σ An/n, An Randomly Equal to ± 1." The Bell System Technical Journal. 52:1097-1103 (September 1973).

11. Jones, J. Jay. "Filter Distortion and Intersymbol Interference Effects on PSK Signals." IEEE Transactions on Communication Technology, COM-19 2:120-132 (April 1971).

12. Johnson, David E. Introduction to Filter Theory. Englewood Cliffs, New Jersey: Prentice-Hall, Inc., 1976.

13. Hansell, Grant E. Filter Design and Evaluation. New York: Van Nostrand Reinhold Company, 1969.

14. Stiffler, J.J. Theory of Synchronous Communications. Englewood Cliffs, New Jersey: Prentice-Hall, Inc., 1971.

15. Lindsey, William C. Synchronization Systems in Communication and Control. Englewood Cliffs, New Jersey: Prentice-Hall, Inc., 1972.

16. Lindsey, William C., and M.K. Simon. Telecommunication Systems Engineering. Englewood Cliffs, New Jersey: Prentice-Hall, Inc., 1973.

Appendix A

Computer Programs

Early in the development of the equations in Chapter II, many common terms were found to exist from one equation to another. For this reason, the major program tasks were written as modules that could be utilized by different driver programs. All programming was written in Fortran IV for use on the CDC-6600 computer system at the Air Force Institute of Technology, Wright-Patterson Air Force Base, Ohio. The following descriptions of the modules or subroutines together with the listings in Tables XII, XIII, and XIV are provided should anyone wish to use these programs for future work.

Subroutine PULSE

Subroutine PULSE computes the pulse-response of an i^{th} datum signal. Ten data intervals of the pulse response are stored, at 0.02 second intervals, in the array P. The subroutine is used by calling it with an integer value (N) which corresponds to the desired datum signal plus one.

Function SR computes the step-response of the Chebyshev filter in subroutine PULSE. The function is used by passing it a real argument which specifies the time for the quantized step-response to be computed (the time values in P range from 0.0 to 10.0 seconds in 0.02 second intervals). The step-response is normalized in terms of BT products as

discussed in Chapter II.

Subroutine DCAVG

This subroutine numerically integrates any point values that are in array PR and stores the result in the two-dimensional array PM. DCAVG is used by first declaring lower and upper limits for the integration (BOT and TOP). These values are passed to DCAVG via common block FOUR. The two calling arguments for DCAVG (I,J) establish the storage location for the value of the integral in PM.

Function FIT. FIT is a polynominial interpolation routine used in DCAVG whenever a numerical value is required by DCADRE that lies between the quantized data values. This function uses INTERP, an Aitken's Kth Degree Polynomial Interpolation routine in the CDC-6600 user library. The degree of the polynomial used for this thesis was three. This choice was arbitrarily made based on the overall smoothness of the pulse-response in Figure 6.

Function DCADRE. DCADRE performs the actual integration in subroutine DCAVG. It is an adaptive Romberg extrapolation routine of the International Mathematical and Statistical Library.

Subroutine BP

This subroutine computes all of the combinatorial possibilities of a binary bit string. It is used by first computing the number of possibilities (KNT = 2**M) where M is the number of bits. The subroutine is called with M and an

integer from 1 to KNT in steps of one. Therefore, this subroutine is called KNT times. The combinatorial possibilities are computed as binary additions of the previous bit pattern plus one. The output is stored in both IZERO (corresponding to logical values of '1' or '0') and IBIT (corresponding to signal values of '1' or '-1').

Additional Programs

The analytical expression for the step-response, as discussed in Chapter II, was obtained by a numerical analysis through the use of POLY and PARTL. These are local Air Force Institute of Technology user programs.

The plots were obtained by using local utility plotting routines on a CALCOMP plotter.

The error function complement was obtained from ERF. This is a McLaurin series or continued fraction expansion routine from the CDC-6600 users library.

Program Notation

The following is a list of the major program variables and arrays and their usage:

BT	=	bandwidth time product
TWPI	=	two times Pi
C(4,4)	=	array holding the coefficients of the Chebyshev filter
X(502) Y(502)	=	arrays for the plots
PR(500)	=	input array for DCAVG (contains portions of the pulse-response or products of pulse-responses

as required); essentially a scratch pad array

P(500) = output array for PULSE (contains pulse-response)

PM(10,10) = output array for DCAVG (contains integral values)

IBIT(M) = bit patterns

TOP = upper limit of the integral in DCAVG

BOT = lower limit of the integral in DCAVG

PHE = phase error in radians

TAU = delay times

Sample Program, QPSK Probability of Error

The program in Table XIII computes the probability of error for QPSK from Equation 17 in Chapter II. This program was used to obtain the plots in Figures 10, 11, and 12 in Chapter III. The program is very straightforward. After initialization, the outermost loop (DO LOOP 1) provides probability of error curves for the three BT products. First, all of the sine and cosine interference terms, as well as the 0^{th} datum pulse, are computed and stored in the two-dimensional array PM. Then nested DO LOOPs (45 and 25) are used to compute all of the combinatorial possibilities for 50 signal-energy-to-noise ratio points; the resulting probability of error values for these points are stored in array Y.

Sample Program, BPSK Phase Error Variance

The program in Table XIV computes the phase error for BPSK from Equation 26 in Chapter II. This program was used to obtain Figure 14 in Chapter III. First, all of the

integral values from the I term of Equation 25 are computed and stored in the two-diminsional array PM; note that the order of integration and summation has been reversed for ease in computation. The logic after statement number 40 is used to compute the phase error variance for QCM if a flag (IQCM≠0) is declared. The average value of I and I^2 is then obtained for all possibilities within the coherence time of the loop (for this thesis equivalent to ten data pulses), and the average phase error variance is computed for 500 signal-energy-to-noise ratio points.

Table XII

Subroutine Listings

```
      SUBROUTINE PULSE(N)
      COMMON/ONE/ BT,IT,TWPI,C(4,4),T,IM,X(502),Y(502),PR(500)
     *,P(500),PM(10,10)
      DIMENSION PT(500)
      DO 10 I=1,500
      XX=I-1
      XX=XX/50
      X(I)=XX
      P(I)=SR(XX)
      IF(XX.LT.1.0)GO TO 10
      XX=XX-1.
      P(I)=P(I)-SR(XX)
 10   CONTINUE
      IF(IM.NE.N)GO TO 15
      CALL PLOTS(IBUF,500,4HPLOT)
      CALLPLOT(0.,-4.,-3) $ CALL PLOT(0.,0.003,-3)
 15   IF(N.EQ.1) RETURN
      ISTRT=(N-1)*50
      IEND=500-ISTRT
      DO 20 J=1,IEND
      PT(J+ISTRT)=P(J)
 20   CONTINUE
      DO 30 J=1,ISTRT
 30   P(J)=0.0
      K=ISTRT+1
      DO 31 J=K,500
 31   P(J)=PT(J)
      IF(N.NE.IM) RETURN
      DO 40 J=1,500
 40   Y(J)=P(J)
      CALL HGRAPH(X,Y,500,ID,1,0,0) $ CALL PLOTE(M)
      IM=0
      RETURN $ END
```

Table XII, continued

```
 FUNCTION SR(XX)
 COMMON/ONE/ BT,IT,TWPI,C(4,4),T,IM,X(502),Y(502),PR(500)
*,P(500),PM(10,10)
 Z=(XX+IT*T)*BT*TWPI
 SR=C(1,1)
*+(C(2,1)*EXP(C(2,2)*Z))*SIN(C(2,3)*Z+C(2,4))
*+(C(3,1)*EXP(C(3,2)*Z))*SIN(C(3,3)*Z+C(3,4))
*+(C(4,1)*EXP(C(4,2)*Z))*SIN(C(4,3)*Z+C(4,4))
 RETURN $ END


 SUBROUTINE DCAVG( I,J)
 COMMON/ONE/BT,IT,TWPI,C(4,4),T,IM,X(502),Y(502),PR(500)
*,P(500),PM(10,10)
 COMMON /FOUR/TOP,BOT
 EXTERNAL FIT
 PM(I,J)=DCADRE(FIT,BOT,TOP,0.,0.0001,ERROR,IER)

 WRITE*,I,J,PM(I,J)
 RETURN $ END

 FUNCTION FIT(XO)
 DIMENSION TEMP(8)
 COMMON/ONE/BT,IT,TWPI,C(4,4),T,IM,X(502),Y(502),PR(500)
*,P(500),PM(10,10)
 CALL INTERP(X,PR,500,3,XO,FIT,TEMP,IER)
 RETURN $ END
```

Table XII, continued

```
      SUBROUTINE BP (M,KNT)
      COMMON /TWO/IBIT(10),IZERO(10)
      DIMENSION ITHRU(3),IDIAG(3)
      DATA (ITHRU(I),I=1,3)/0,1,0/
      DATA (IDIAG(I),I=1,3)/0,0,1/
      IF(KNT.NE.1)GO TO 10
      DO 5 J=1,M
5     IZERO(J)=0
      GO TO 15
10    IADND=1
      ICARRY=0
      DO 20 J=1,M
      ICARRY=IZERO(J)+ IADND+ICARRY
      IZERO(J)=ITHRU(ICARRY+1)
      ICARRY=IDIAG(ICARRY+1)
      IADND=0
20    CONTINUE
15    KNT=KNT+1
      DO 30 J=1,M
      IBIT(J)=IZERO(J)
      IF(IBIT(J).EQ.0) IBIT(J)=-1
30    CONTINUE

      RETURN $ END
```

Table XIII
QPSK Sample Program

```
      PROGRAM PULSEM(INPUT,OUTPUT,PLOT)
      REAL IDATA,IDD,IDSQ,ISI
     *,ISIC,ISIS
      DIMENSION IO(17),IBUF(500)
     *,BTT(3)
     *,TAU(3),IDAT(3)


      COMMON/ONE/ BT,II,TWPI,C(4,4),T,IM,X(502),Y(502),PR(500)
     *,P(500),PM(10,10)
      COMMON /TWO/ IBIT(19),IZERO(19)
      COMMON /THREE/ ID
      COMMON/FOUR/TOP,BOT
      DATA((C(I,J),I=1,4),J=1,4)/1.,0.34211,0.25237,2.3205,0,-0.31334,
     *-0.11469,-0.42806,0,0.77339,1.0555,0.28310,0,2.0275,-.34430,
     *4.0028/
      DATA (TAU(I),I=1,3)/0.74,0.52,0.38/,(IDAT(I),I=1,3)/2,2,2/
     *,(BTT(I),I=1,3)/1.,1.5,2./
      IT=0 $ T=1. $ TWPI=6.283185307
      PHE=0.0 $ NO=-1
      CALL FMT1
      CALL PLOTS(IBUF,1024,4HPLOT)
      CALLPLOT(0.,-4.,-3) $ CALL PLOT(0.,0.03,-3)
      DO 1 I=1,3
      II=1 $ BT=BTT(I)
      CALL PULSE(II)
      DO 2 J=1,500
    2 PR(J)=P(J)
      J=1 $ BOT=0.0 $ TOP=AMOD(TAU(I),1.)
    5 CALL DCAVG(J,1)
      IF(J.EQ.10)GO TO 10
      J=J+1 $ BOT=TOP $ TOP=TOP+1 $ GO TO 5
   10 DO 6 J=1,10
```

Table XIII, continued

```
6       PM(J,2)=PM(J,1)
        PMTMP=PM(IDAT(I),1)
        ISTP=10-IDAT(I)
        DO 20  J=1,ISTP
        I3=J+IDAT(I)  $  I2=I3-1
20      PM(I2,1)=PM(I3,1)
        PM(10,1)=PMTMP
        WRITE*,PM
        DO 45  ISNR=1,50
        SNR=ISNR+1  $  SNR=SNR/2
        KNT=1  $  IBITT=9
        ISTOP=2**IBITT
        PER=0.
        DO 25  J=1,ISTOP

        CALL  BP(IBITT,KNT)
        ISIC=0.  $  ISIS=0.
        DO 30  JJ=1,4
30      ISIC=(PM(JJ,1)*IBIT(JJ))+ISIC
        DO 35  JJ=1,5
35      ISIS=(PM(JJ,2)*IBIT(JJ+9))+ISIS
        ARG=(SNR**0.5)*(COS(PHE)*(PM(10,1)+ISIC)+SIN(PHE)*ISIS)
        CALL  ERF(ARG,0,DU,PERT)
25      PER=PER+PERT
        PER=PER/1024.
        PER=(PER*2.)-(PER**2.)  $  Y(ISNR)=PER  $  X(ISNR)=10*ALOG10(SNR)
        WRITE*,PER,X(ISNR)
45      CONTINUE
        X(51)=0.  $  X(52)=15./4.9  $  Y(51)=1.0E-12  $  Y(52)=12./7.
        CALL  VLGRAF(X,Y,50,ID,NO,0,0)  $  ND=2
1       CONTINUE
        CALL  PLOTE(M)  $  STOP  $  END
```

Table XIV

BPSK Phase Error Variance Program

```
      PROGRAM PULSEM(INPUT,OUTPUT,PLOT)
      REAL IDATA,IDD,IDSQ
      DIMENSION ID(17),IBUF(500)


      COMMON/ONE/ BT,IT,TWPI,C(4,4),T,IM,X(502),Y(502),PR(500)
     *,P(500),PM(10,10)
      COMMON /TWO/ IBIT(10),IZERO(10)
      COMMON /THREE/ ID
      DATA((C(I,J),I=1,4),J=1,4)/1.,0.94211,0.25237,2.3205,0,-0.31334,
     *-0.11469,-0.42806,0,0.77339,1.0565,0.28310,0,2.0275,-.34430,
     *4.0028/
      CALL FMT1
      BT=0.5 $ IT=0 $ T=1. $ TWPI=6.283185307
      IOCM=0
      DO 1 IBT=1,4
      IF(IBT.EQ.4)GO TO 31
      I=1
      J=1
10    CALL PULSE(I)
      DO 25 K=1,500
25    PR(K)=P(K)
      IF(I.EQ.J) GO TO 30
      CALL PULSE(J)
      DO 35 K=1,500
35    PR(K)=PR(K)*P(K)
      GO TO 40
30    DO 45 K=1,500
45    PR(K)=PR(K)*PR(K)
40    CALL DCAVG( I, J)
      IF(IOCM.EQ.0)GO TO 41
      ITEST=MOD((I+J), 2)
      IF(ITEST.EQ.1)PM(I,J)=0.0
```

Table XIV, continued

```
      WRITE*,I,J,PM(I, J)
41    CONTINUE
      IF(I.EQ.10) GO TO 50
      I=I+1
      GO TO 10
50    IF(J.EQ.10) GO TO 60
      J=J+1
      I=J
      GO TO 10
60    CONTINUE
      IDD=0.0 $ IDSQ=0.0 $ IEND=2**10
      ISTRT=1
65    CALL BP(10,ISTRT)
      I=2 $ J=1 $ IDATA=0.0
70    IDATA=(2*IBIT(I)*IBIT(J))*PM(I,J)+IDATA
      IF(I.NE.10) GO TO 71
      IF(J.NE.9) GO TO 72
      IF(IEND.EQ.1024) WRITE*,IDATA
      GO TO 73
71    I=I+1 $ GO TO 70
72    J=J+1 $ I=J+1 $ GO TO 70
73    DO 75 J=1,10
75    IDATA=PM(J,J)+IDATA
      IDD=IDATA+IDD
      IDSQ=IDATA*IDATA+IDSQ
      IEND=IEND-1
      IF(IEND.EQ.1023) WRITE*,IDD,IDSQ,3T
      IF(IEND.NE.0) GO TO 65
      WRITE*,IDD,IDSQ
      IDD=1/(IDD/(2**10))
      IDSQ=(1/(IDSQ/(2**10)))/2
31    IF(IBT.NE.4)GO TO 32
      IDD=1.0 $ IDSQ=1.0
32    SNR=1.0
      DO 80 J=1,500
```

Table XIV, continued

```
      Y(J)=(((1./SNR)**2)*IDSQ)+((1./SNR)*IDD)
      X(J)=10*ALOG10(SNR)
80    SNR=SNR+0.2
      X(502)=3.0 $ Y(502)=0.6
      IF(IBT.NE.1)GO TO 2
      CALL PLOTS(IBUF,500,4HPLOT)
      CALL PLOT(0.,-4.,-3) $ CALL PLOT(0.,0.003,-3)
      IP=-1
2     CALL FMT2

      CALL HGRAPH(X,Y,500,ID,IP,0,0)
      BT=BT+0.5
1     IP=2
      CALL PLOTE(M)
      STOP $ END
```

VITA

Gary A. White was born on 16 November 1942 in Kansas City, Missouri. He graduated from Olathe High School, Olathe, Kansas and enlisted into the United States Air Force in 1960. His enlisted duties were as a Link trainer instructor and a weather equipment technician. In 1970, he entered the Airman Educationing and Commissioning Program and was graduated from Texas A&M with a B.S. in Meteorology in May, 1972. After attending Officer Training School, he received a commission in the USAF. He was a Weather Officer (AFSC 2524) at Air Force Global Weather Central, (AFGWC) Offutt AFB, Nebraska. There he worked as a program designer and analyst on various numerical weather prediction models and applications programs, including the meteorological portion of the Strategic Automated Command and Control System (SACCS). He was also a System Duty Officer for the five Univac 1100 series computers during his last year at AFGWC. In 1975 he entered the Postgraduate Engineering Sciences program at the Air Force Institute of Technology. In 1976, he was selected to continue in the Graduate Electrical Engineering program. Captain White is a member of Chi Epsilon Pi, Phi Kappa Phi, Tau Beta Pi, Eta Kappa Nu, and is the current President of the Student Council, AFIT School of Engineering.

Permanent Address: 300 No. Chestnut, Apt. 306
Olathe, Kansas 66061

UNCLASSIFIED

SECURITY CLASSIFICATION OF THIS PAGE (When Data Entered)

REPORT DOCUMENTATION PAGE	READ INSTRUCTIONS BEFORE COMPLETING FORM
1. REPORT NUMBER AFIT/GE/EE/77-37 2. GOVT ACCESSION NO.	3. RECIPIENT'S CATALOG NUMBER
4. TITLE (and Subtitle) QUADRATURE CLOCK MODULATION VERSUS BINARY AND QUADRATURE PHASE SHIFT KEYING IN THE PRESENCE OF INTERSYMBOL INTERFERENCE	5. TYPE OF REPORT & PERIOD COVERED MS Thesis
	6. PERFORMING ORG. REPORT NUMBER
7. AUTHOR(s) Gary A. White Captain	8. CONTRACT OR GRANT NUMBER(s)
9. PERFORMING ORGANIZATION NAME AND ADDRESS Air Force Institute of Technology (AFIT-EN) Wright-Patterson AFB, Ohio 45433	10. PROGRAM ELEMENT, PROJECT, TASK AREA & WORK UNIT NUMBERS
11. CONTROLLING OFFICE NAME AND ADDRESS Defense Communication Engineering Center/ R420 1860 Wiehle Ave. Reston, Virginia 22091	12. REPORT DATE December 1977
	13. NUMBER OF PAGES 89
14. MONITORING AGENCY NAME & ADDRESS(if different from Controlling Office)	15. SECURITY CLASS. (of this report) UNCLASSIFIED
	15a. DECLASSIFICATION/DOWNGRADING SCHEDULE

16. DISTRIBUTION STATEMENT (of this Report)

Approved for public release; distribution unlimited

17. DISTRIBUTION STATEMENT (of the abstract entered in Block 20, if different from Report)

18. SUPPLEMENTARY NOTES

Approved for public release; IAW AFR 190-17

JERRAL F. GUESS, Captain, USAF
Director of Information

19. KEY WORDS (Continue on reverse side if necessary and identify by block number)

Quadrature Clock Modulation
Binary Phase Shift Keying
Quadrature Phase Shift Keying
Intersymbol Interference
Data Communication
Carrier Tracking

20. ABSTRACT (Continue on reverse side if necessary and identify by block number)

Quadrature Clock Modulation (QCM) is a binary phase shift keying (BPSK) technique in which alternate bits are transmitted orthogonally. Compared to normal BPSK modulation, QCM improves the performance of a communication system which is limited by intersymbol interference (ISI). Compared to quadrature phase shift keying (QPSK) for the same information rates, QCM is slightly inferior in data detection performance. The average

DD FORM 1 JAN 73 1473 EDITION OF 1 NOV 65 IS OBSOLETE

UNCLASSIFIED

SECURITY CLASSIFICATION OF THIS PAGE (When Data Entered)

012 225

(20. cont.)

carrier tracking capability of a QCM scheme is equal to that of BPSK for the same closed-loop bandwidth and time bandwidth product (BT) of the channel filter at a specified signal energy to noise ratio (Eb/No).

The data detection performance for QCM, BPSK, and QPSK is analyzed by comparing the one-shot probability of error conditioned on a phase error as a function of Eb/No and BT for a specified channel filter. Carrier tracking performance for QCM and BPSK is analyzed by obtaining an average phase error variance for the linear model of a Costas loop. In computing both the probability of error and phase error variance, the intersymbol interference is modeled from a truncated data sequence. In addition, the bit energy penalty for tracking a QPSK signal versus a BPSK or QCM signal with no ISI is examined.